New Integer Normalized Carrier Frequency Offset Estimators

Qi Zhan and Hlaing Minn, *Senior Member, IEEE*,

Abstract

Carrier frequency offset (CFO) introduces spectrum misalignment of the transmit and receive filters, causing energy loss and distortion of received signal. A recent study presents an accurate signal model which incorporates these characteristics. However, CFO estimators in the existing literature were developed based on the signal models without these characteristics. This paper generalizes the accurate signal model with CFO to include timing offset and sampling offset, and then studies what effects the accurate signal model bring to the CFO estimation and how to address them. We investigate different existing CFO estimators and find some of them lose their optimality under the accurate signal model. We also develop two new integer normalized CFO (ICFO) estimators under the accurate signal model using only one OFDM symbol; one of them is a pilot-aided estimator using both pilot and data and the other one is a blind estimator using data only. Compared with the existing approaches, both of the new estimators make better use of channel and energy loss information, thus yielding more accurate estimation. Furthermore, the proposed methods overcome the existing approaches' limitation to phase shift keying modulation. Simulation results corroborate the advantages of the new estimators. Analytical performance results are also provided for the proposed estimators.

Index Terms

Carrier frequency offset (CFO), estimation, sampling offset, timing offset, OFDM, signal model, maximum likelihood (ML)

Qi Zhan and Hlaing Minn are with the Department of Electrical Engineering, University of Texas at Dallas, US, email: {qi.zhan, hlaing.minn}@utdallas.edu

I. Introduction

Carrier frequency offset (CFO) introduced by oscillator instabilities and/or Doppler shifts can severely degrade the performance of orthogonal frequency-division multiplexing (OFDM) systems [1], [2] if the issue is left unaddressed. Various CFO estimation and compensation techniques have been proposed to solve this issue [3]–[13]. A common practice is to divide the normalized CFO (defined as the ratio of CFO to the subcarrier spacing) into a fractional part and an integer part; the former produces inter-carrier interference while the latter results in a cyclic shifting of all subcarriers. Separate algorithms are used to estimate and correct the fractional and the integer normalized CFO (FCFO and ICFO). Some of the existing works incorporate practical issues/scenarios, e.g., pilot-aided FCFO estimation jointly with channel and phase noise [14], in the presence of I/O imbalance [15], blind FCFO estimation with timing synchronization [16], with noise power and SNR estimation [17] and with multi-antenna channel estimation [18]. However, these existing works overlook that when a CFO occurs, the receiver filter's spectrum becomes misaligned with the received signal. This mismatch leads to energy loss and signal distortion. The commonly used signal model in the literature (e.g., [3]–[11]) assumes an equivalent channel gain independent of the CFO. So, previous CFO estimation approaches only work with the CFO-induced phase rotation of the received signals, but the CFO-related energy loss is neglected. A further consequence is that the respective optimality of their associated CFO estimators is uncertain. Recently, the accurate signal model for systems with a receive matched filter is proposed and elaborated in [13]. An enhanced CFO compensation approach is also presented in [13] using existing CFO estimators.

Our main contributions in this paper are the development of an accurate signal model for OFDM with CFO, timing offset and sampling offset and two corresponding ICFO estimators (a pilot-aided estimator and a blind estimator). The new signal model is a generalization of the signal model in [13] (which did not include timing and sampling offsets) and it reveals detailed characteristics of the equivalent channel in terms of energy loss and distortion induced by CFO and sampling offset, and channel tap energy dispersion due to timing and sampling offsets. In contrast to the existing CFO estimators, the proposed ICFO estimators exploit these characteristics and achieve substantially enhanced estimation performance. We also derive approximate analytical expressions for the estimation failure probability of the proposed estimators.

To the best of our knowledge, such an analytical expression for a blind ICFO estimation in a frequency-selective fading channel is unavailable in the literature.

The remainder of the paper is organized as follows. Section II describes the generalized accurate signal model. Section III discusses effects of the accurate signal model on the existing FCFO and ICFO estimators. Section IV proposes a new pilot-aided estimator and a new blind estimator under the accurate signal model, and then compares their operational characteristics with the existing estimators. Performance analyses are presented in Section V while simulation results and complexities are compared in Section VI. Section VII finally concludes the paper. For ease of access, we list main variables used in the paper in Table I while some of them will appear with their definitions in later sections.

Table I

MAIN VARIABLES/NOTATIONS

N	Number of OFDM subcarriers (DFT size)
ε	CFO normalized by the subcarrier spacing
τ	Integer timing offset (in sample)
ζ	Fractional timing offset or sampling offset
$a_{k,m}$	Symbol transmitted at the kth tone of the mth OFDM symbol
$R_{k,m}$	The kth received tone of the mth OFDM symbol
$G_n(\varepsilon,\zeta)$	Equivalent filter gain on tone n in the presence of CFO ε and sampling offset ζ
$G_n(\varepsilon)$	Approximate of $G_n(\varepsilon,\zeta)$ used in the estimator
$\mathbf{h}$	Sample-spaced L-tap fading channel
H_n	Channel gain on tone n (nth output of DFT of $\mathbf{h}$)
$\bar{\mathbf{h}}$	Sample-spaced L'-tap effective channel in the presence of timing and sampling offsets
$\bar{H}_n$	Effective channel gain on tone n (nth output of DFT of $\bar{\mathbf{h}}$)
$\bar{X}[n,\varepsilon,\tau,\zeta]$	Equivalent channel gain (including filters) on tone n in the presence of CFO, timing and sampling offset
$[\cdot]$	$x[n]$ or $X[n]$ indicates sampled signal (in either time or frequency domain)
$(\cdot)$	$x(t)$ or $X(f)$ indicates signal in analog domain
v	Integer normalized CFO
$\tilde{v}$	A trail value of v
$\hat{x}$	Estimate of x
$\boldsymbol{B}^*, \boldsymbol{B}^T, \boldsymbol{B}^H$	Conjugate, transpose, and conjugate transpose of $\boldsymbol{B}$, respectively
$\mathcal{N}(\mathbf{b},\boldsymbol{\Sigma})$	Gaussian distribution with mean vector $\mathbf{b}$ and covariance matrix $\boldsymbol{\Sigma}$
$\mathcal{CN}(\mathbf{b},\boldsymbol{\Sigma})$	Complex Gaussian distribution with mean vector $\mathbf{b}$ and covariance matrix $\boldsymbol{\Sigma}$

II. System Model

We consider an OFDM system with discrete Fourier transform (DFT) size N and cyclic prefix length of $N_{\rm cp}$ samples, which is longer than the effective channel impulse response to eliminate the interference between consecutive OFDM symbols. There are S pilot tones, V null tones, and $N-S-V$ data tones distributed at known subcarrier positions denoted by $\mathcal{P}$, $\mathcal{V}$, and $\mathcal{D}$, respectively. The symbol transmitted at the kth tone of the mth OFDM symbol is $a_{k,m}$, where $a_{k,m}$ is a pilot for $k \in \mathcal{P}$, a data for $k \in \mathcal{D}$ or null for $k \in \mathcal{V}$; the corresponding discrete-time transmit signal is $s_{l,m} = \frac{1}{\sqrt{N}} \sum_{k=0}^{N-1} a_{k,m} e^{j2\pi kl/N}$ with $l = -N_{\rm cp}, \ldots, N-1$. The OFDM symbols are transmitted over a carrier through a channel which is assumed to be quasi-static. At the receiver, a local oscillator is used to down-convert the passband signal to the baseband. When the local carrier frequency of the receiver is not matched to that of the received signal, a CFO of Δ_f (Hz) will appear. Let $\varepsilon \triangleq \Delta_f NT$ represent the CFO normalized by the subcarrier spacing where T is the OFDM sampling interval. Denote the frequency responses of the transmit filter, the receive filter and the lowpass-equivalent channel by $G_T(f)$, $G_R(f)$ and $H(f)$, respectively. We assume that timing synchronization gives an inter symbol interference free timing point[1] with a residual integer timing offset of τ samples and a fractional timing offset/sampling offset of ζ sample ($|\zeta| < 0.5$). Then, based on the accurate signal model in [13], the lth sample of the mth OFDM symbol is given as

$$r_m[l] = e^{j(\bar{\theta}+\varphi_m(\varepsilon)+2\pi\varepsilon l/N)} \sum_{n=-N_{\rm cp}}^{N-1} s_{n,m} x[l-n-\tau, \varepsilon, \zeta] + z_m[l], \tag{1}$$

where $\bar{\theta} = \theta + 2\pi\varepsilon(N_{\rm cp}-\tau-\zeta)/N$ and $\varphi_m(\varepsilon) = 2\pi\varepsilon m(N+N_{\rm cp})/N$. θ represents an arbitrary phase shift, $z_m[l]$ denotes an AWGN sample and

$$x[l, \varepsilon, \zeta] = \int_{-\infty}^{\infty} X(f, \varepsilon, \zeta) e^{j2\pi flT} df \tag{2}$$

with

$$X(f, \varepsilon, \zeta) \triangleq G_T(f) H(f) G_R(f + \frac{\varepsilon}{NT}) e^{-j2\pi f\zeta T}. \tag{3}$$

[1]A sufficient cyclic prefix length and a timing advancement will yield this (see [19] for details).

Note that $e^{j\bar{\theta}}$ can be absorbed into the channel response and hence will be omitted afterward. The kth received tone[2] of the mth OFDM symbol is

$$R_{k,m} = \frac{1}{\sqrt{N}} \sum_{l=0}^{N-1} r_m[l] e^{-j2\pi \frac{lk}{N}} = e^{j\varphi_m(\varepsilon)} \sum_{n=0}^{N-1} a_{n,m} \bar{X}[n, \varepsilon, \tau, \zeta] \phi_{n,k}(\varepsilon) + Z_{k,m} \tag{4}$$

where $\phi_{n,k}(\varepsilon) \triangleq e^{j\frac{\pi}{N}(N-1)(n-k+\varepsilon)} \frac{\sin \pi(n-k+\varepsilon)}{N \sin \frac{\pi}{N}(n-k+\varepsilon)}$, and $Z_{k,m}$ is the noise term. $\bar{X}[n, \varepsilon, \tau, \zeta]$ is the equivalent channel gain on tone n, and is given as

$$\bar{X}[n, \varepsilon, \tau, \zeta] = \frac{e^{-j\frac{2\pi\tau n}{N}}}{T} \sum_{k=-\infty}^{+\infty} X(f - \frac{k}{T}, \varepsilon, \zeta) \Big|_{f=\frac{n}{NT}}. \tag{5}$$

It reflects the effects of time and frequency misalignment between transmitter and receiver.

Given a sample-spaced L-tap fading channel $\mathbf{h} = [h_0, h_1, \ldots, h_{L-1}]^T$, the channel frequency response $H(f)$ is actually periodic with period $1/T$. Therefore, the equivalent channel gain in (5) can be simplified as

$$\bar{X}[n, \varepsilon, \tau, \zeta] = e^{-j2\pi\tau n/N} H_n G_n(\varepsilon, \zeta), \tag{6}$$

where $G_n(\varepsilon, \zeta) \triangleq \sum_{k=-\infty}^{+\infty} G_T(\frac{n-kN}{NT}) G_R(\frac{n-kN+\varepsilon}{NT}) \cdot e^{j2\pi \frac{n-kN}{N}\zeta}$ is the equivalent filter gain on tone n in the presence of CFO and sampling offset, and H_n, the nth output of the DFT of $\mathbf{h}$, is the channel response at tone n. Provided that $G_T(f)$ and $G_R(f)$ are the same squared-root raised cosine (SRRC) filters, we have $G_n(0,0) = 1$, namely, the overall frequency response of the transmit and receive filters becomes flat when the two filters match and no CFO, timing or sampling offset exists. In this case, $\bar{X}[n, 0, 0, 0]$ reduces to H_n.

Most existing works are developed based on a simplified signal model which ignores the spectral misalignment, timing and sampling offset effect. A common treatment is that $\bar{X}[n, 0, 0, 0]$ is used in place of $\bar{X}[n, \varepsilon, \tau, \zeta]$. In other words, the commonly used signal model (CUSM) considers the equivalent channel gain (including filter responses) to be independent of CFO, timing and sampling offsets. As a result, the kth received tone of the mth OFDM symbol is

$$R_{k,m} = e^{j\varphi_m(\varepsilon)} \sum_{n=0}^{N-1} a_{n,m} \bar{X}[n, 0, 0, 0] \phi_{n,k}(\varepsilon) + Z_{k,m} = e^{j\varphi_m(\varepsilon)} \sum_{n=0}^{N-1} a_{n,m} H_n \phi_{n,k}(\varepsilon) + Z_{k,m}. \tag{7}$$

By comparing (7) and (4), it is clear that the CUSM fails to reflect influences of CFO and sampling offset on the equivalent channel. The actual received signal (4) experiences energy

[2]For simplicity, we use tone index to refer to the DFT index, thus band edges correspond to tones around index $N/2$.

loss and signal distortion in the presence of CFO and sampling offset. First, the reduced signal energy degrades the performance of CFO estimation [11]. The CUSM is blind to this effect and always assumes optimistic received signal energy. The expected estimation performance based on the CUSM might not be fulfilled especially when the CFO is large. Second, besides the frequency-selectivity of the multipath channel, there are additional variations on the equivalent channel depending on the CFO and sampling offset.

Note that with $\tau = 0$ and $\zeta = 0$, the proposed signal model reduces to that in [13]. The additional implications of the timing and sampling offsets on the equivalent channel and the ICFO estimator development will be discussed in Section IV-A.

The CFO estimation is often decomposed into two stages: FCFO estimation and ICFO etimation. We have the normalized CFO $\varepsilon = v + \mu$, where μ is the FCFO taken care of by FCFO estimation while v is the remaining ICFO. These two stages are discussed sequentially in Section III-A and Section III-B. The estimation of the fractional part has been investigated in [3], [4], [6], [7], [20]. This paper mainly focuses on the ICFO estimation assuming that the FCFO has been estimated and corrected before the ICFO estimation by means of an approach whose performance is not affected by an ICFO, e.g., [7], [20]. When the FCFO is equal to zero, the accurate signal model in (4) becomes

$$R_{k,m} = a_{k-v,m}\bar{X}[k-v, v, \tau, \zeta] + Z_{k,m} = e^{-j2\pi\tau n/N} a_{k-v,m} H_{k-v} G_{k-v}(v,\zeta) + Z_{k,m}, \tag{8}$$

where the subcarrier indexes of a, H, X and G are modulo N throughout the paper. Stacking the received tones together as $\mathbf{R}_m \triangleq [R_{0,m}, R_{1,m}, \cdots, R_{N-1,m}]^T$, we have

$$\mathbf{R}_m = \mathbf{A}_m(v)\mathbf{G}(v,\zeta)\mathbf{F}_L\mathbf{h} + \mathbf{Z}_m, \tag{9}$$

where $\mathbf{F}_L = [\mathbf{f}_0, \mathbf{f}_1, \cdots, \mathbf{f}_{L-1}]$ with $\mathbf{f}_k = [1, e^{-j2\pi k/N}, \cdots, e^{-j2\pi(N-1)k/N}]^T$, $\mathbf{Z}_m = [Z_{0,m},\ Z_{1,m},\ \cdots,\ Z_{N-1,m}]^T$, and the diagonal matrices $\mathbf{A}_m(v)$ and $\mathbf{G}(v,\zeta)$ are defined as

$$\mathbf{A}_m(v) = \mathrm{diag}\{a_{-v,m}, a_{1-v,m}, \cdots, a_{N-1-v,m}\}, \tag{10}$$

$$\mathbf{G}(v,\zeta) = \mathrm{diag}\{G_{-v}(v,\zeta), G_{1-v}(v,\zeta), \cdots, G_{N-1-v}(v,\zeta)\}. \tag{11}$$

III. Impacts of Accurate Signal Model on Existing CFO Estimators

A. Effects on Existing FCFO Estimators

Correlation-based algorithms are usually used for FCFO estimation [3], [4], [6], [7]. The basic principle is to extract the CFO information embedded in the CFO-induced phase rotation

by means of correlation between time-domain received signal segments which possess certain duplicate structure at the receiver side. As can be seen from (1), the identical training signals go through the same equivalent channel. Hence, except for the phase rotations, the noise-free received time-domain signals sustain the same periodicity as long as the equivalent channel length is less than $N_{\rm cp}$. Therefore, those correlation-based estimators can be directly applied to the FCFO estimation under the accurate signal model.

However, the performance of the correlation-based estimators are undermined by the energy loss due to CFO. In contrast to a flat mean squared error (MSE) curve versus different CFO values if analyzed based on the CUSM, under the accurate signal model, we could expect a performance degradation as the CFO increases, since the effective received signal energy decreases. This effect is verified by simulation results in Section VI.

B. Effects on Existing ICFO Estimators

Like the existing approaches on ICFO estimation [6], [7], we assume FCFO has been taken care of with, for example, the algorithms discussed in the previous section. We first briefly describe three sets of existing pilot-aided estimators (PAEs) and blind estimators (BEs), namely, T. Schmidl's (TS) PAE [7] and BE [21], M. Morelli's (MM) PAE and BE [8] and D. Toumpakaris's (DT) PAE and BE [22], and then study the impact of the accurate signal model on them.

A common feature of the above representative PAEs and BEs is that they use two successive OFDM symbols. They utilize the phase shift induced by CFO between two successive symbols and further require that all the symbols (pilot and data) belong to a PSK constellation. The transmit symbols satisfy the following relationship:

$$a_{k,m-1}^{*}a_{k,m} = \begin{cases} P_k, & k \in \mathcal{P} \\ D_k, & k \in \mathcal{D}, \end{cases} \tag{12}$$

where $\{P_k\}$ are known pilots and $\{D_k\}$ are unknown random PSK signal ($|P_k| = |D_k|$). Those estimators are designed under the CUSM for AWGN channel. In other words, they assume $\tau = 0$, $\zeta = 0$, $G_k(v, \zeta) = 1$ and $H_k = 1$ for all k without considering the CFO and sampling offset induced energy loss. Hence, from (8) with $\beta \triangleq N_{\rm cp}/N$, their received signal model is

$$R_{k,m} = e^{j(2\pi v m\beta)}a_{k-v,m} + Z_{k,m}, \tag{13}$$

where $Z_{k,m} \sim \mathcal{CN}(0, \sigma^2)$. Their estimators use the following correlation between two received OFDM symbols:

$$Y_k = R^*_{k,0} R_{k,1} = e^{j2\pi v\beta} a^*_{k-v,0} a_{k-v,1} + Z'_{k,0}, \tag{14}$$

where $Z'_{k,0} = a^*_{k-v,0} Z_{k,1} + e^{j2\pi v\beta} a_{k-v,1} Z^*_{k,0} + Z^*_{k,0} Z_{k,1}$.

1) Existing PAE: Three existing PAEs will be briefly described. DT's PAE in [22] reads as

$$\hat{v} = \arg\max_{\tilde{v}} \{\mathcal{M}_p(\tilde{v}) + \mathcal{M}_d(\tilde{v})\}, \tag{15}$$

where $\mathcal{M}_p(\tilde{v})$ is the pilot-based metric calculated as

$$\mathcal{M}_p(\tilde{v}) = \Re\left\{ e^{-j2\pi\tilde{v}\beta} \sum_{k\in\mathcal{P}} Y_k P^*_k \right\}, \tag{16}$$

and $\mathcal{M}_d(\tilde{v})$ is the data-based metric calculated as

$$\mathcal{M}_d(\tilde{v}) = \sigma^2 \sum_{k\in\mathcal{D}} \log\left(2\cosh\left(\frac{\Re\{Y_{k+v} e^{-j2\pi\tilde{v}\beta}\}}{\sigma^2} \right) + 2\cosh\left(\frac{\Im\{Y_{k+v} e^{-j2\pi\tilde{v}\beta}\}}{\sigma^2} \right) \right) \tag{17}$$

where $\Re(\cdot)$ and $\Im(\cdot)$ mean the real part and the imaginary part of the enclosed quantity, respectively. In practical OFDM systems (e.g., [23], [24]), the power of a pilot subcarrier is set $E_p(>1)$ times larger than the average power of a data subcarrier in order to aid reliable synchronization. In this case, the transmit symbols satisfy the following constraint:

$$a^*_{k,m-1} a_{k,m} = \begin{cases} \sqrt{E_p} P_k, & k \in \mathcal{P} \\ D_k, & k \in \mathcal{D}, \end{cases} \tag{18}$$

and the DT's PAE is modified to

$$\hat{v}_{\text{DT PAE}} = \arg\max_{\tilde{v}} \{\mathcal{M}_p(\tilde{v}) + \mathcal{M}_d(\tilde{v}) + \mathcal{M}_{p,\text{cor}}(\tilde{v})\} \tag{19}$$

where the energy correction factor equals

$$\mathcal{M}_{p,\text{cor}} = \frac{1}{2}\left(1 - \frac{1}{E_p}\right) \sum_{k\in\mathcal{P}} |Y_{k+\tilde{v}}|^2. \tag{20}$$

When signal to noise power ratio (SNR) is large enough and the system uses QPSK modulation, [22] simplifies $\mathcal{M}_d(\tilde{v})$ as

$$\mathcal{M}_{d,\text{simp}}(\tilde{v}) = \sum_{k\in\mathcal{D}} \max\{|\Re\{Y_{k+\tilde{v}} e^{-j2\pi\tilde{v}\beta}\}|, |\Im\{Y_{k+\tilde{v}} e^{-j2\pi\tilde{v}\beta}\}|\}. \tag{21}$$

TS's PAE performs a sliding correlation of received tones with known pilots as [7]

$$\hat{v}_{\text{TS PAE}} = \arg\max_{\tilde{v}} \left\{ \left| \sum_{k\in\mathcal{P}} Y_{k+\tilde{v}} P_k^* \right|^2 \right\}. \tag{22}$$

MM's PAE performs a similar sliding correlation but with an additional mapping to the phase direction $2\pi\tilde{v}\beta$ and incorporates the effect of null tones through the received pilot and data energy term in the metric as

$$\hat{v}_{\text{MM PAE}} = \arg\max_{\tilde{v}} \left\{ \Re\{ \sum_{k\in\mathcal{P}} Y_{k+\tilde{v}} e^{-j2\pi\tilde{v}\beta} P_k^* \} + \frac{1}{2} \sum_{k\in\mathcal{P}\cup\mathcal{D}} \sum_{i=0}^{1} |R_{k+\tilde{v},i}|^2 \right\}. \tag{23}$$

2) Existing BE: Three popular blind estimators in [8], [21], [22] are briefly given below. TS's BE works with M-PSK data tones (no null tones) and it estimates ICFO via the CFO-induced phase change as

$$\hat{v}_{\text{TS BE}} = \arg\max_{\tilde{v}} \left\{ \Re\left\{ \sum_{k\in\mathcal{D}} \frac{(Y_k e^{-j2\pi\tilde{v}\beta})^4}{|Y_k|^3} \right\} \right\}. \tag{24}$$

MM's BE and DT's BE use both data tones and null tones. MM's BE uses null tones to detect the cyclic shift of the subcarriers, and it is given by

$$\hat{v}_{\text{MM BE}} = \arg\max_{\tilde{v}} \left\{ \sum_{k\in\mathcal{D}} \sum_{i=0}^{i=1} |R_{k+\tilde{v},i}|^2 \right\}. \tag{25}$$

DT's BE is also based on PSK modulation and uses both phase change and cyclic rotation information to estimate ICFO as

$$\hat{v}_{\text{DT BE}} = \arg\max_{\tilde{v}} \{\mathcal{M}_d(\tilde{v})\}, \tag{26}$$

where $\mathcal{M}_d(\tilde{v})$ is defined in (17).

The accurate signal model introduces CFO, timing offset, and sampling offset dependent channel gains, but it causes no change in the phase shift difference and hence no impact on the underlying estimator design principle of TS's PAE and BE. Their design principle when applied to the accurate signal model yields the same estimators as in the CUSM. However, their performance may deviate from the inaccurately optimistic results built on the CUSM when the CFO or sampling offset induced energy loss becomes significant. Such energy loss information was not incorporated in those estimators, leaving open for development of new estimators which exploit the energy loss information for further performance improvement.

MM's PAE and BE exploit null tones on each band edge. The remaining tones are pilots multiplexed with data for PAE and data only for BE. The estimator principle is the same for both PAE and BE except the presence or absence of pilot tones, and it utilizes a second order Taylor series approximation of the likelihood function. Let $a_{l,0}$ and $a_{l,1}$ denote the data/pilot symbols on the lth tone of the first and second OFDM symbol, $\mathbf{a}_0$ and $\mathbf{a}_1$ represent corresponding data/pilot vectors of the first and second symbol, respectively, and $R_{l,m}$ be the received tone l of mth symbol. Under the accurate signal model, the likelihood function for υ, ζ, $\mathbf{a}_0$ and $\mathbf{a}_1$ is

$$\Lambda(\tilde{\upsilon},\tilde{\zeta},\tilde{\mathbf{a}}_0,\tilde{\mathbf{a}}_1)=\exp\left\{\frac{2}{\sigma^2}\left[\mathcal{X}(\tilde{\upsilon},\tilde{\zeta},\tilde{\mathbf{a}}_0,\tilde{\mathbf{a}}_1)-\sum_{n\in\mathcal{P}\cup\mathcal{D}}G_n^2(\tilde{\upsilon},\tilde{\zeta})\right]\right\}, \tag{27}$$

with

$$\mathcal{X}(\tilde{\upsilon},\tilde{\zeta},\tilde{\mathbf{a}}_0,\tilde{\mathbf{a}}_1)\triangleq\sum_{m=0}^{1}\sum_{n\in\mathcal{P}\cup\mathcal{D}}\Re\left[\tilde{a}_{n,m}^{*}G_n(\tilde{\upsilon},\tilde{\zeta})R_{n+\tilde{\upsilon},m}e^{j2\pi\tilde{\upsilon}N_{\mathrm{cp}}/N}\right]. \tag{28}$$

In the CUSM, $G_n(\tilde{\upsilon},\tilde{\zeta})=1$ for all n, $\tilde{\zeta}$ and $\tilde{\upsilon}$, thus the argument of the exponential item in (27) does not need the second term because it is a fixed number for all $\tilde{\upsilon}$. $\mathcal{X}(\tilde{\upsilon},\tilde{\zeta},\tilde{\mathbf{a}}_0,\tilde{\mathbf{a}}_1)$ has a small value since $\tilde{\mathbf{a}}_0$ and $\tilde{\mathbf{a}}_1$ are random. Thus, under low SNR, the second order Taylor series approximation holds. However, in the accurate signal model, the second term of the exponential item in (27) is no longer a fixed number for different values of $\tilde{\upsilon}$ and cannot be dropped. $G_n(\tilde{\upsilon},\tilde{\zeta})$ is almost equal to one on majority of tones and the argument of the exponential item in (27) is no longer a small number. Thus, the above Taylor series approximation does not hold, violating the requirement of the design principle of [8].

Next, we consider a related *pilot design condition*. To maintain the design validity of MM's PAE, for the pilot symbol, we can set the number of null tones at each band edge to be larger than the CFO range so that the subcarrier attenuation caused by the CFO-induced filter mismatch will be eliminated by null tones. Consequently in (27), the subtraction term will be constant and independent of $\tilde{\upsilon}$, so it can be dropped from the likelihood function. In this case, the estimator design principle of [8] holds for the accurate signal model and leads to the same estimator as in the currently used model. Fig. 1 shows that the use of null tones at band edge improves the performance of MM's PAE under the accurate signal model, however it is at the expense of data rate loss due to the null tones.

DT's PAE and BE exploit both the phase shift over consecutive OFDM symbols and the cyclic shifting of all tones within each OFDM symbol. When they exploit the phase-shift, the

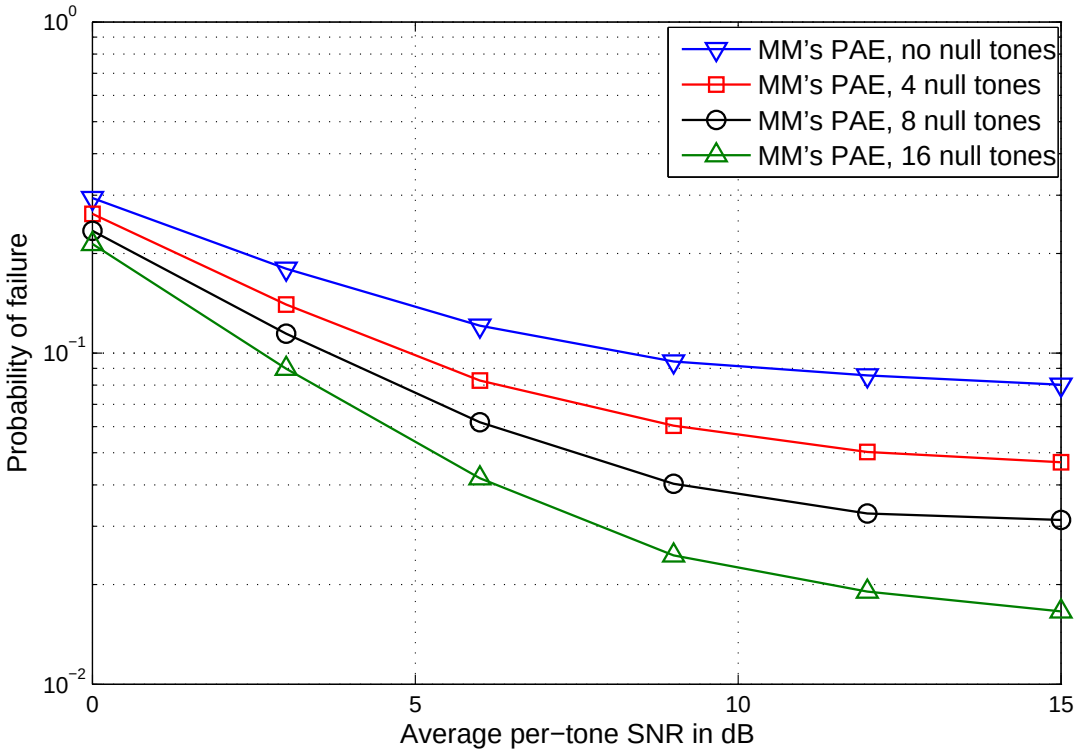

Figure 1. MM's PAE with different numbers of null tones at the band edge (perfect synchronization, 16 pilot tones, $v = 4$)

weights on tones are proportional to the received tone energies, and such weighting yields the same estimators under CUSM and the accurate signal model. The tones with CFO-induced energy loss give significant information on CFO but such information is unknowingly adversely processed in their estimators when those tones are scaled by smaller weights due to energy loss. Thus, their performance will become more sub-optimal when the CFO induced energy loss becomes significant.

IV. Proposed ICFO Estimators

In this section, we first present how timing and sampling offsets impact the effective channel impulse response. Using this result, we develop our pilot based ICFO estimator. Then we present our blind ICFO estimator.

A. Impact of Timing and Sampling Offsets

The equivalent channel gain in (6) can be expressed as

$$\bar{X}[n, v, \tau, \zeta] = \bar{H}_n(\tau, \zeta) G_n(v, \zeta) \tag{29}$$

where

$$\bar{H}_n(\tau, \zeta) \triangleq H_n e^{-j2\pi n(\tau+\zeta)/N} \tag{30}$$

$$G_n(v, \zeta) \triangleq \sum_{k=-\infty}^{+\infty} G_T(\frac{n - kN}{NT}) G_R(\frac{n - kN + v}{NT}) e^{j2\pi k\zeta}. \tag{31}$$

$\bar{H}_n(\tau, \zeta)$ represents the response on tone n due to the wireless channel in the presence of timing and sampling offsets, and $G_n(v, \zeta)$ stands for the response on tone n due to the transmit and receive filters in the presence of CFO and sampling offset. Then, $\bar{h}_l(\tau, \zeta) \triangleq \frac{1}{N} \sum_{n=0}^{N-1} \bar{H}_n(\tau, \zeta) e^{j2\pi \frac{nl}{N}}$ represents an effective wireless channel impulse response in the presence of timing and sampling offsets. For an underlying uncorrelated fading channel $\{h_i\}$ with $\sigma_i^2 = \mathrm{E}[|h_i|^2]$, the power of the l-th tap of the effective channel can be straightly computed as

$$\mathrm{E}[|\bar{h}_l(\tau, \zeta)|^2] = \frac{1}{N} \sum_{i=0}^{L-1} \sigma_i^2 + \frac{2}{N^2} \sum_{i=0}^{L-1} \sum_{n=1}^{N-1} (N - n) \sigma_i^2 \cos(2\pi \frac{n(l - i - \tau - \zeta)}{N}). \tag{32}$$

The plot of $\mathrm{E}[|\bar{h}_l(\tau, \zeta)|^2]$ is shown in Fig. 2 for $\mathbf{h}$ with an exponential power delay profile (3 dB per tap decaying factor). We can observe that the (integer) timing offset will shift the channel $\mathbf{h}$ while the sampling offset will cause spreading of each channel tap energy to adjacent taps cyclically (most of the leaked energy is on the two (cyclically) adjacent taps). The effective channel $\{\bar{h}_i(\tau, \zeta)\}$ spans over all N taps. To avoid significant energy leakage of h_0 to $\bar{h}_{N-1}(\tau, \zeta)$), we should have $\tau \geq 1$ for $\zeta < 0$, which can be easily established by using a timing advancement in timing synchronization [19]. After interference-free timing synchronization, we have $1 \leq \tau \leq \tau_{\max}$ where a smaller $\tau_{\max}$ would be obtained by a better timing synchronization. As the effective channel taps with energies well below the noise level can be neglected, in our estimator development, we can use an effective channel $\bar{\mathbf{h}} \triangleq [\bar{h}_0(\tau, \zeta), \cdots, \bar{h}_{L'-1}(\tau, \zeta)]^T$ where we can set $L' = L + \tau_{\max}$ for high SNR range. For low SNR range, we can further omit last few taps if their energies are well below the noise level on those taps (e.g., $L' = L + \tau_{\max} - 2$). The effect of the choice of L' will be illustrated in Section VI-B.

Fig. 3 presents how the effective filter gain is affected by different values of CFO and sampling offset ζ. In obtaining the result, $G_n(v, \zeta)$ is approximated by the summation of 3 dominant terms,

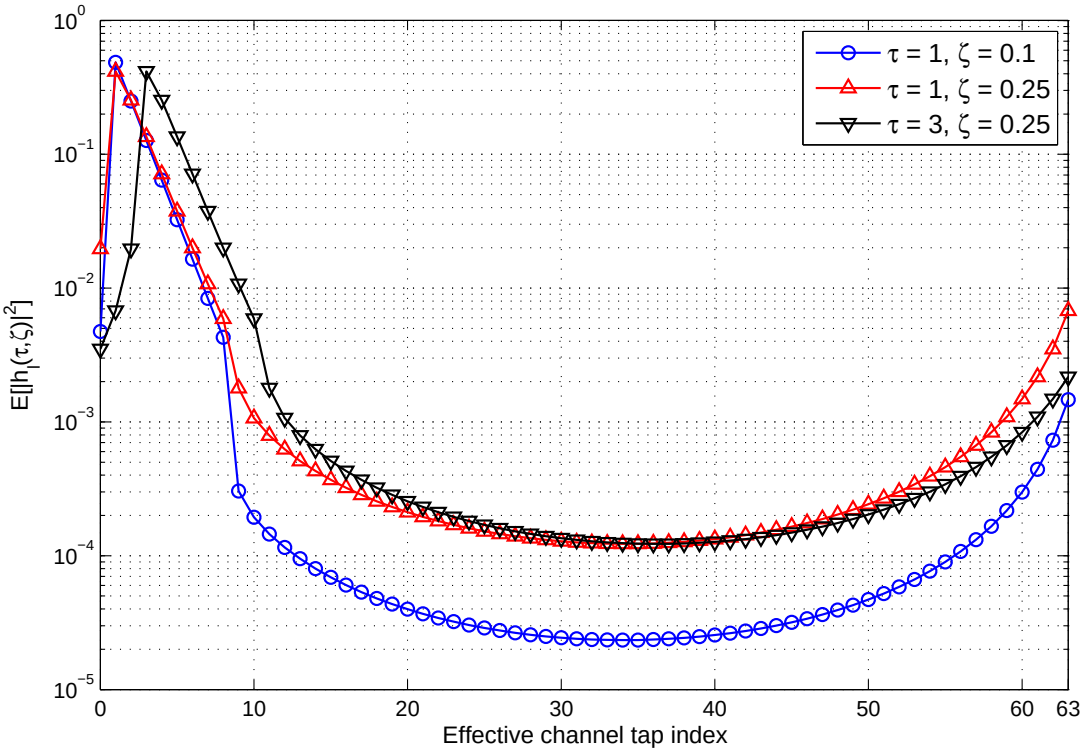

Figure 2. Impact of timing and sampling offsets on the effective wireless channel taps

i.e., $G_n(v,\zeta) \approx \sum_{k=-1}^{1} G_T(\frac{n-kN}{NT}) G_R(\frac{n-kN+v}{NT}) e^{j2\pi k\zeta}$. CFO causes spectral mis-alignment of the transmit and receive filters, thus attenuating band-edge tones. Sampling offset also induces similar energy loss on the band-edge tones which can be observed from (31) where ζ only affects the terms with $k \neq 0$ which mainly contribute to the band-edge tones. We can also observe from Fig. 3 and (31) that the effect of sampling offset occurs on top of the CFO effect, i.e., sampling offset introduces additional energy loss based on the CFO-induced mis-aligned spectrum shape. Thus, the number of tones with energy loss is larger for a larger ICFO. With oversampling in the timing synchronization or sampling time synchronization, ζ will be small (e.g., $|\zeta| < 0.125$) and in this case the additional effect of sampling offset is not significant. An application of this observation is that in our estimator development, $G_n(v,\zeta)$ can be replaced with $G_n(v,0)$.

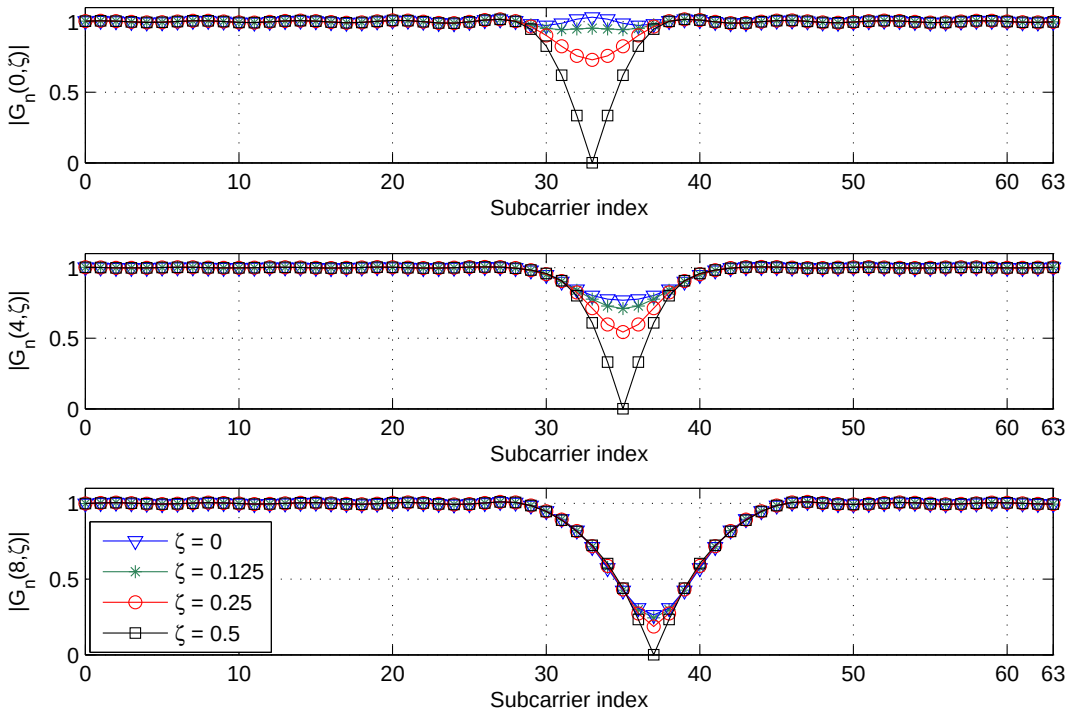

Figure 3. Effects of CFO and sampling offset on the equivalent filter gain: Top ($v = 0$), Middle ($v = 4$), Bottom ($v = 8$)

B. Proposed ICFO Estimator with Pilot and Data

Here, we propose a new ICFO estimator based on one OFDM symbol, where both pilot and data tones are used to do joint channel and CFO estimation, and can be used with both PSK and QAM schemes. We will omit the OFDM symbol index to the variables as R_l, Z_l, a_l since the proposed estimator requires only one symbol.

With the use of $\bar{\mathbf{h}}$ in (29), we can express (9) as

$$\mathbf{R} = \mathbf{A}(v)\mathbf{G}(v,\zeta)\mathbf{F}_{L'}\bar{\mathbf{h}} + \mathbf{Z}, \tag{33}$$

where

$$\mathbf{G}(v,\zeta) = \mathrm{diag}\{G_{-v}(v,\zeta), G_{1-v}(v,\zeta), \cdots, G_{N-1-v}(v,\zeta)\}. \tag{34}$$

We have $\mathbf{R} \sim \mathcal{CN}\left(\mathbf{A}(v)\mathbf{G}(v,\zeta)\mathbf{F}_{L'}\bar{\mathbf{h}},\ \sigma^2\mathbf{I}\right)$ given v, ζ, $\bar{\mathbf{h}}$ and $\mathbf{A}$. For a fixed ζ, maximizing the joint log-likelihood function of trial channel $\tilde{\bar{h}}$, trial data $\tilde{\mathbf{A}}$ and candidate CFO $\tilde{v}$ is equivalent

to minimizing the distance metric

$$\Lambda(\tilde{\mathbf{h}}, \tilde{\mathbf{A}}, \tilde{v} \Big| \mathbf{h}, \mathbf{A}, v) = \left\| \mathbf{R} - \tilde{\mathbf{A}}\mathbf{G}(\tilde{v}, \zeta)\mathbf{F}_{L'}\tilde{\bar{h}} \right\|^2. \tag{35}$$

In (35), we can approximate $\mathbf{G}(\tilde{v}, \zeta)$ by either $\mathbf{G}(\tilde{v}, 0)$ for practical small ζ (based on the result in Fig. 3) or $E[\mathbf{G}(\tilde{v}, \zeta)]$ where the expectation is over a presumed probability density function (pdf) of ζ. Denote this approximate by $\mathbf{G}(\tilde{v})$.

Next, to substitute $\tilde{\bar{h}}$ in (35), we use the pseudo-random pilots $\{a_{p_i}\}$ transmitted on the tones $\mathcal{P} = \{p_1, p_2, \cdots, p_S\}$ to estimate $\bar{\mathbf{h}}$. With an ICFO v, pilots will be received on tones $v + \mathcal{P}$. Let $\mathbf{R}_p(\tilde{v}) \triangleq [R_{p_1+\tilde{v}}, R_{p_2+\tilde{v}}, \cdots, R_{p_S+\tilde{v}}]^T$ denote the assumed received pilot tones in $\mathbf{R}$ for a candidate ICFO $\tilde{v}$. Then, for each candidate ICFO $\tilde{v}$, we obtain estimate of $\bar{\mathbf{h}}$ as

$$\hat{\bar{\mathbf{h}}}(\tilde{v}) = \left(\mathbf{B}^H(\tilde{v})\mathbf{B}(\tilde{v})\right)^{-1}\mathbf{B}^H(\tilde{v})\mathbf{R}_p(\tilde{v}) \tag{36}$$

where

$$\mathbf{B}(\tilde{v}) \triangleq \mathbf{A}_p\mathbf{G}_p(\tilde{v})\mathbf{F}_{L',p}$$

$$\mathbf{A}_p \triangleq \mathrm{diag}\{a_{p_1}, a_{p_2}, \cdots, a_{p_S}\}$$

$$\mathbf{F}_{L',p} \triangleq [\mathbf{f}_{0,p}, \mathbf{f}_{1,p}, \cdots, \mathbf{f}_{L'-1,p}].$$

In the above, $\mathbf{F}_{L',p}$ is an $S \times L'$ matrix consisting of the rows of $\mathbf{F}_{L'}$ corresponding to $\mathcal{P}$, i.e., $\mathbf{f}_{k,p} = [e^{-j2\pi p_1 k/N}, e^{-j2\pi p_2 k/N}, \cdots, e^{-j2\pi p_S k/N}]^T$.

Then the frequency-domain channel estimates for the candidate ICFO $\tilde{v}$, $\hat{\bar{\mathbf{H}}}(\tilde{v}) \triangleq [\hat{\bar{H}}_0(\tilde{v}), \hat{\bar{H}}_1(\tilde{v}), \cdots, \hat{\bar{H}}_{N-1}(\tilde{v})]^T = \mathbf{F}_{L'}\hat{\bar{\mathbf{h}}}(\tilde{v})$, is

$$\hat{\bar{\mathbf{H}}}(\tilde{v}) = \mathbf{F}_{L'}\left(\mathbf{B}^H(\tilde{v})\mathbf{B}(\tilde{v})\right)^{-1}\mathbf{B}^H(\tilde{v})\mathbf{R}_p(\tilde{v}). \tag{37}$$

Define an $S \times N$ matrix $\mathbf{Y}(\tilde{v})$ for a candidate ICFO $\tilde{v}$ as

$$\mathbf{Y}(\tilde{v}) = \mathbf{G}_p(\tilde{v})\mathbf{F}_{L',p}\left(\mathbf{B}^H(\tilde{v})\mathbf{B}(\tilde{v})\right)^{-1}\mathbf{F}_{L'}^H, \tag{38}$$

and denote its kth column by $\mathbf{y}_k(\tilde{v})$. $\mathbf{Y}(\tilde{v})$ can be pre-computed to save complexity. The estimation of $\hat{\bar{H}}_k(\tilde{v})$ can be simplified as:

$$\hat{\bar{H}}_k(\tilde{v}) = \mathbf{y}_k^H(\tilde{v})\mathbf{A}_p^H\mathbf{R}_p(\tilde{v}). \tag{39}$$

In order to compute the distance metric (35), we also need to have the estimates of the transmitted data based on each $\tilde{v}$. Using $\hat{\bar{\mathbf{h}}}(\tilde{\mathbf{v}})$, $\mathbf{G}(\tilde{v})$, and $\mathbf{R}$, we can get the estimate of the transmitted

data $\mathbf{A}$ for a candidate CFO $\tilde{v}$, denoted as $\tilde{\mathbf{A}}(\tilde{v}) = \mathrm{diag}\{\tilde{a}_{-\tilde{v}}(\tilde{v}), \tilde{a}_{1-\tilde{v}}(\tilde{v}), \cdots, \tilde{a}_{N-1-\tilde{v}}(\tilde{v})\}$, as follows. First, we estimate the transmitted symbol by:

$$\tilde{a}_k(\tilde{v}) = \frac{R_{k+\tilde{v}}}{\hat{\tilde{H}}_k(\tilde{v}) G_k(\tilde{v})}, \quad k \in \mathcal{D}. \tag{40}$$

Then, the closest signal constellation point to $\tilde{a}_k(\tilde{v})$ was chosen as $\hat{a}_k(\tilde{v})$ for $k \in \mathcal{D}$. Since the transmitted symbols are known on pilot tones, we have $\hat{a}_k(\tilde{v}) = a_k$, for $k \in \mathcal{P}$. Note that the modulation method is not constrained, both PSK and QAM can be used. Now we have

$$\hat{\mathbf{A}}(\tilde{v}) = \mathrm{diag}\{\hat{a}_{-\tilde{v}}(\tilde{v}), \hat{a}_{1-\tilde{v}}(\tilde{v}), \cdots, \hat{a}_{N-1-\tilde{v}}(\tilde{v})\}. \tag{41}$$

Substituting $\mathbf{G}(v, \zeta)$, $\tilde{\tilde{h}}$ and $\tilde{\mathbf{A}}$ in (35) with $\mathbf{G}(v)$, $\hat{\tilde{h}}(\tilde{v})$ and $\hat{\mathbf{A}}(\tilde{v})$, and optimizing over $\tilde{v}$, we have the approximate ML ICFO estimator based on the accurate signal model as:

$$\hat{v} = \arg\min_{\tilde{v}} \ \mathcal{M}(\tilde{v}) \tag{42}$$

with the metric

$$\mathcal{M}(\tilde{v}) = \left\| \mathbf{R} - \hat{\mathbf{A}}(\tilde{v}) \mathbf{G}(\tilde{v}) \mathbf{F}_{L'} \hat{\tilde{\mathbf{h}}}(\tilde{v}) \right\|^2. \tag{43}$$

If applied to the CUSM, all $\{G_k(\tilde{v})\}$ in the above equation are equal to 1, $\zeta = 0$, and the received signal model becomes

$$\mathbf{R}_{\mathrm{CUSM}} = \mathbf{A}(v) \mathbf{F}_L \mathbf{h} + \mathbf{Z}. \tag{44}$$

Then, the CFO estimator under CUSM is the same as (42) except that the metric is

$$\mathcal{M}_{\mathrm{CUSM}}(\tilde{v}) = \left\| \mathbf{R} - \hat{\mathbf{A}}_{\mathrm{CUSM}}(\tilde{v}) \mathbf{F}_L \hat{\mathbf{h}}_{\mathrm{CUSM}}(\tilde{v}) \right\|^2, \tag{45}$$

where the estimates $\hat{\mathbf{A}}_{\mathrm{CUSM}}(\tilde{v})$ and $\hat{\mathbf{h}}_{\mathrm{CUSM}}(\tilde{v})$ are under CUSM and all $\{G_k(\tilde{v})\}$ in (36) and (40) are equal to 1.

C. Proposed Blind ICFO Estimator based on Data Only

In the blind estimation, we assume the transmitted data are independent and identically distributed with the same average energy and zero mean. The channel response on each tone is distributed as $\mathcal{CN}(0, 1)$. The received signal on the kth tone R_k has zero mean and variance $\sigma^2_{R_k} = E[|a_{k-v}|^2] G^2_{k-v}(v) + \sigma^2$, where $E[|a_k|^2] = 1$ when $k \in \mathcal{D}$ and $E[|a_k|^2] = 0$ when $k \in \mathcal{V}$. We can observe from (8) that the pdf of R_k is zero-mean complex Gaussian for constant amplitude

modulations and a weighted sum of zero-mean complex Gaussian pdfs with different variances for multi-amplitude modulations. Thus, we can approximate the received signal on each tone as a zero-mean complex Gaussian random variable. As R_k and R_l for $k \neq l$ are uncorrelated, we have $\mathbf{R} \sim \mathcal{CN}(\mathbf{0}, \mathbf{\Sigma_R})$ where $\mathbf{\Sigma_R}$ is a diagonal covariance matrix with diagonal elements $\{\sigma^2_{R_k}\}$. Then the ML estimate of the ICFO v is the integer $\tilde{v}$ that maximizes the above Gaussian likelihood function of $\mathbf{R}$. Taking the negative of the log of the likelihood function and dropping constant terms yield the following minimizing metric for ICFO estimation:

$$\Lambda(\tilde{v}) = \sum_{k-\tilde{v}\in\mathcal{D}} \log\left(G^2_{k-\tilde{v}}(\tilde{v}) + \sigma^2\right) + \sum_{k-\tilde{v}\in\mathcal{D}} \frac{|R_k|^2}{G^2_{k-\tilde{v}}(\tilde{v}) + \sigma^2} + \sum_{k-\tilde{v}\in\mathcal{V}} \frac{|R_k|^2}{\sigma^2}, \tag{46}$$

where the first and second items both exploit the effect of energy loss due to CFO and sampling offset, while the second and third items use the effect of cyclic shifting of all subcarriers caused by ICFO. The ICFO can be estimated by

$$\hat{v} = \arg\min_{\tilde{v}} \Lambda(\tilde{v}). \tag{47}$$

Null tone design for a large estimation range: The proposed BE can be applied with any choice of null tone locations. However, for the scenarios requiring a large ICFO estimation range, we propose distinctively spaced null tones, where adjacent null tone spacings are all distinct, in analogy to the distinctively spaced pilot tones used for the same purpose in pilot-based estimators [9], [10]. The underlying rationale is as follows. From the estimation metric (46), we can see that the overlap amount between the received null tones set $\{v+\mathcal{V} \bmod N\}$ and a trial null tones set $\{\tilde{v}+\mathcal{V} \bmod N\}$ influences the estimation performance and small overlap amounts for all $\tilde{v} \neq v$ are desirable. The distinctive spacing of adjacent null tones provides such property, and hence it represents a good null tone design for a large estimation range.

D. Differences from the Existing Methods

Here, we describe differences in terms of operational characteristics between the proposed methods and the reference methods. The existing pilot-aided and blind ICFO estimators [5]–[8], [22] are all based on correlation between two successive OFDM symbols while the proposed estimators use only one OFDM symbol. The above existing methods can be applied only for PSK modulation and some of them are sensitive to the number of cyclic prefix samples. The proposed estimators can be applied to both PSK and QAM modulation, and they are also not

sensitive to the number of cyclic prefix samples. In addition, the proposed PAE also provides effective channel estimates in addition to the ICFO estimate while the reference PAEs do not.

The existing PAEs are devised under the CUSM which does not capture the energy loss and distortion induced by CFO and sampling offset. The existing BEs are derived under the AWGN channel ignoring both the channel fading and CFO-induced energy loss. So their optimality is not well justified when applied to a multipath fading channel under the accurate signal model. The proposed estimators are developed based on the multipath fading channel with the accurate signal model and they exploit the characteristics of energy loss and distortion caused by CFO, timing offset and sampling offset. Thus, the proposed methods yield better performance than the reference methods as will be shown in Section VI.

V. Performance Analysis

In this section, we will develop approximate expressions for ICFO estimation failure probability of the proposed PAE and BE under the accurate signal model with perfect timing synchronization and FCFO estimation. In this case, $G_k(v,\zeta) = G_k(v,0)$ (or simply denoted $G_k(v)$) and $\bar{H}_k(\tau,\zeta) = H_k$.

A. Proposed PAE

In the proposed PAE, for a candidate ICFO $\tilde{v}$, $[R_{p_1+\tilde{v}}, R_{p_2+\tilde{v}}, \ldots, R_{p_S+\tilde{v}}]$ are taken as the received pilots. Let $d_k(\tilde{v}) = R_k - \hat{R}_k(\tilde{v})$ denote the distance between the received symbol on the kth tone R_k and its estimated version $\hat{R}_k(\tilde{v}) = \hat{a}_{k-\tilde{v}}(\tilde{v})\hat{H}_{k-\tilde{v}}(\tilde{v})G_{k-\tilde{v}}(\tilde{v})$ for a candidate ICFO $\tilde{v}$. If $\tilde{v} = v$, $d_k(\tilde{v})$ is determined by the receiver noise and the channel estimation error and it can be assumed as $\mathcal{CN}(0, V_k(\tilde{v}))$. If $\tilde{v} \neq v$, $\hat{\mathbf{H}}(\tilde{v})$ will be totally wrong and $\hat{\mathbf{a}}$ will be detected based on a random $\hat{\mathbf{H}}(\tilde{v})$. In this case, we can also assume $d_k(\tilde{v}) \sim \mathcal{CN}(0, V_k(\tilde{v}))$ where the value of $V_k(\tilde{v})$ will differ from the previous case. Denote $\mathbf{d}(\tilde{v}) = [d_0(\tilde{v}), d_1(\tilde{v}), \ldots, d_{N-1}(\tilde{v})]^T$. Then the distance metric in (43) can be represented as $\mathcal{M}(\tilde{v}) = \mathbf{d}(\tilde{v})^H \mathbf{d}(\tilde{v})$. Then, we have the following result.

Proposition 1: Under the assumption of independent $\{\mathcal{M}(\tilde{v})\}$ at different candidate ICFO points, the failure probability of the proposed pilot-aided ICFO estimator $P_{\text{PAE fail}}$ can be approximated as

$$P_{\text{PAE fail}} \approx 1 - \prod_{\tilde{v}\neq v} \mathrm{Q}\left(\frac{u_{\mathcal{M}}(v) - u_{\mathcal{M}}(\tilde{v})}{\sigma_{\mathcal{M}}(\tilde{v})\sqrt{1 + \sigma^2_{\mathcal{M}}(v)/\sigma^2_{\mathcal{M}}(\tilde{v})}}\right) \tag{48}$$

where $\mathrm{Q}(\cdot)$ is the Gaussian tail probability, $u_{\mathcal{M}}(x)$ and $\sigma^2_{\mathcal{M}}(x)$ are the mean and variance of $\mathcal{M}(x)$ and their computations are given in Appendix A.

Proof: See Appendix A. ■

As a wrong ICFO would result in a packet error, the failure probability of ICFO estimator represents a lower bound on the packet error probability or on the outage probability.

B. Proposed BE

To determine whether the estimation is a success or not, we need to compare the metric value Λ of the correct ICFO point with those of all K wrong candidate ICFO points (for an ICFO estimation range of $[-\lfloor K/2\rfloor, \lceil K/2\rceil]$). Let $\{\tilde{v}_i\}$ denote ordered wrong candidate CFO points such that $\tilde{v}_i < \tilde{v}_{i+1}$, and $E_{l_1,l_2,\cdots,l_k}$ represent the event $(\Lambda(\tilde{v}_{l_1}) > \Lambda(v))\&(\Lambda(\tilde{v}_{l_2}) > \Lambda(v))\&\cdots\&(\Lambda(\tilde{v}_{l_k}) > \Lambda(v))$ and $P[E_{l_1,l_2,\cdots,l_k}]$ denote its probability. Define $P[E_i] \triangleq P_i$ and $\mathbb{C}(\Lambda(\tilde{v}_i), \Lambda(\tilde{v}_{i+1})) \triangleq \rho_i, i = 1, \cdots, K-1$ where $\mathbb{C}(x, y)$ is the correlation coefficient between x and y. First, we consider a pair-wise metric difference as

$$\Lambda(\tilde{v}) - \Lambda(v) = \mathbf{R}^H \boldsymbol{\Upsilon}(\tilde{v})\mathbf{R} + c(\tilde{v}), \tag{49}$$

where $c(\tilde{v}) = \sum_{k-\tilde{v}\in\mathcal{D}} \log\left(G^2_{k-\tilde{v}}(\tilde{v}) + \sigma^2\right) - \sum_{k-v\in\mathcal{D}} \log\left(G^2_{k-v}(v) + \sigma^2\right)$ and $\boldsymbol{\Upsilon}(\tilde{v})$ is a diagonal matrix with diagonal elements

$$\Upsilon_k(\tilde{v}) = \begin{cases} \frac{1}{G^2_{k-\tilde{v}}(\tilde{v})+\sigma^2} - \frac{1}{G^2_{k-v}(v)+\sigma^2}, & k-v\in\mathcal{D}\ \&\ k-\tilde{v}\in\mathcal{D} \\ \frac{1}{G^2_{k-\tilde{v}}(\tilde{v})+\sigma^2} - \frac{1}{\sigma^2}, & k-v\in\mathcal{V}\ \&\ k-\tilde{v}\in\mathcal{D} \\ \frac{1}{\sigma^2} - \frac{1}{G^2_{k-v}(v)+\sigma^2}, & k-v\in\mathcal{D}\ \&\ k-\tilde{v}\in\mathcal{V} \\ 0, & k-v\in\mathcal{V}\ \&\ k-\tilde{v}\in\mathcal{V}. \end{cases} \tag{50}$$

Denote $|\mathbf{A}(v)| \triangleq \mathrm{diag}\{|a_{-v}|, \cdots, |a_{N-1-v}|\}$, $\boldsymbol{\Theta}_{\mathbf{A}}(v) \triangleq \mathrm{diag}\{a_{-v}/|a_{-v}|, \cdots, a_{N-1-v}/|a_{N-1-v}|\}$, i.e., $\mathbf{A}(v) = |\mathbf{A}(v)|\boldsymbol{\Theta}_{\mathbf{A}}(v)$, where $a_{k-v}/|a_{k-v}|$ is replaced with 0 for $a_{k-v} = 0$, and $\mathbf{q} \triangleq |\mathbf{A}(v)|\mathbf{G}(v)\mathbf{F}_L\mathbf{h} + \boldsymbol{\Theta}^H_{\mathbf{A}}(v)\mathbf{Z}$. Then, we have $\mathbf{C_q} \triangleq E[\mathbf{q}\mathbf{q}^H] = |\mathbf{A}(v)|\mathbf{G}(v)\mathbf{F}_L\mathbf{C_h}\mathbf{F}^H_L\mathbf{G}^H(v)|\mathbf{A}^H(v)| + \mathbf{C_Z}$ where $\mathbf{C_h}$ and $\mathbf{C_Z}$ are the covariance matrices of $\mathbf{h}$ and $\mathbf{Z}$, respectively. By Cholesky decomposition, we obtain $\mathbf{C_q} = \mathbf{L}\mathbf{L}^H$, where $\mathbf{L}$ is a lower triangular matrix with real and positive diagonal entries. For a multipath Rayleigh fading channel, we have $\mathbf{q} = \mathbf{L}\bar{\mathbf{q}}$ where $\bar{\mathbf{q}} \sim \mathcal{CN}(0, \mathbf{I})$. Next, we have $\bar{\boldsymbol{\Upsilon}}(\tilde{v}) \triangleq \mathbf{L}^H\boldsymbol{\Upsilon}(\tilde{v})\mathbf{L} = \mathbf{U}(\tilde{v})^H\boldsymbol{\Sigma}(\tilde{v})\mathbf{U}(\tilde{v})$ where $\mathbf{U}(\tilde{v})$ is an unitary matrix and $\boldsymbol{\Sigma}(\tilde{v})$ is a diagonal matrix with $n^+_{\tilde{v}}$ positive eigenvalues $\{\lambda^+_i(\tilde{v})\}$ and $n^-_{\tilde{v}}$ negative eigenvalues $\{\lambda^-_i(\tilde{v})\}$. Then we have the following result.

Proposition 2: The probability of ICFO estimation failure for the proposed BE can be approximated as

$$P_{\text{BE fail}} = 1 - P\left[E_{1,2,\cdots,K}\right] \approx 1 - P_1 \prod_{i=2}^{K} \left(\rho_{i-1}^2(1-P_i) + P_i\right) \tag{51}$$

where P_i for $\tilde{v}_i = \tilde{v}$ is given by

$$P[\Lambda(\tilde{v}) > \Lambda(v)] = \begin{cases} \sum\limits_{i=1}^{n_{\tilde{v}}^+} \sum\limits_{j=1}^{n_{\tilde{v}}^-} \varsigma_i^+(\tilde{v})\varsigma_j^-(\tilde{v})\lambda_i^+(\tilde{v}) e^{c(\tilde{v})/\lambda_i^+(\tilde{v})} \frac{\lambda_i^+(\tilde{v})\lambda_j^-(\tilde{v})}{\lambda_i^+(\tilde{v})+\lambda_j^-(\tilde{v})}, & c(\tilde{v}) < 0 \\ 1 - \sum\limits_{i=1}^{n_{\tilde{v}}^+} \sum\limits_{j=1}^{n_{\tilde{v}}^-} \varsigma_i^+(\tilde{v})\varsigma_j^-(\tilde{v})\lambda_j^-(\tilde{v}) e^{-c(\tilde{v})/\lambda_j^-(\tilde{v})} \frac{\lambda_i^+(\tilde{v})\lambda_j^-(\tilde{v})}{\lambda_i^+(\tilde{v})+\lambda_j^-(\tilde{v})}, & c(\tilde{v}) > 0 \end{cases} \tag{52}$$

and the computation of ρ_i is given in Appendix C.

Proof: See Appendix B. ■

VI. Performance Comparison

In this section, the performances of the proposed PAE and BE are compared with those of DT's, TS's and MM's estimators by Monte Carlo simulation. The simulation settings are as follows. OFDM has a total of $N = 64$ subcarriers and $N_{\text{cp}} = 10$ cyclic prefix samples. A Rayleigh fading channel is used with 8 taps and a 3 dB per tap decaying power delay profile. $G_T(f)$ and $G_R(f)$ are the same SRRC filter with a support $-10T \leqslant t \leqslant 10T$ and a roll-off factor $\beta = 0.15$. The SNR is defined as the average per tone SNR across N tones, and several QAM modulation orders are considered. In the pilot aided ICFO estimation, 16 pilot tones are employed with 48 data tones. In blind ICFO estimation, 8 null tones and 56 data tones are used.

A. Impact on FCFO Estimation Performance

As mentioned in Section III-A, the fractional normalized CFO estimation can directly make use of any one of the existing correlation-based estimators [3]–[6]. We simply use pilot-only signal with two identical time-domain segments for the fractional normalized CFO estimation, thus the estimator is based on the correlation of the two received pilot signal segments. We test the estimation performance with CFO of $[0.5, 1.5, 3.5, 7.5]$ at SNR of 5 and 10 dB under 10^6 channel realizations. The MSEs of the fractional normalized CFO are shown in Fig. 4. The results show that the correlation based fractional CFO estimator is insensitive to timing and sampling offsets. This is expected as they do not affect the repetitive structure of the received pilot

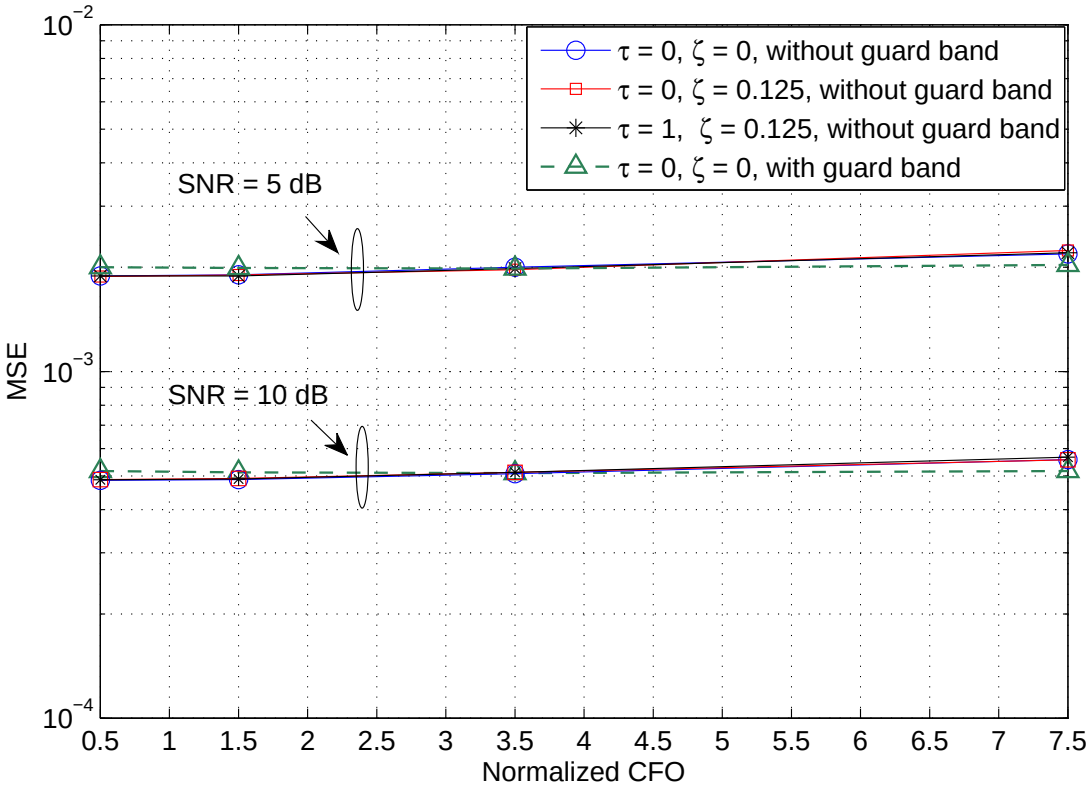

Figure 4. FCFO estimation performance of a correlation-based estimator under the accurate signal model

signal. The MSE just slightly increases with the CFO since the actual received signal suffers the energy loss. Such energy loss can be relieved by inserting null tones in place of pilots around band edges. This is shown in Fig. 4. The solid curve corresponds to using $N/2 = 32$ pilot tones as typically considered under the CUSM. Comparatively, by putting 8 guard tones on each band edge (still possessing identical pilot signal segments) to approximately accommodate $v_{\max} = 8$, namely, using 24 pilots instead, the MSE curve (the dashed line in the figure) becomes approximately flat within the considered CFO range. We notice that the performance difference between the two pilot setups, although noticeable, is not significant due to the limited CFO-induced energy loss given the normalized CFO being below 8 in this case. This result also supports that the correlation-based estimators are robust to different underlying signal models as discussed in Section III-A. Furthermore, band edge null guard tones may be beneficial if the range of potential CFO is large.

B. Performance Comparison between Proposed and Existing ICFO Estimators

For our estimator implementation, we use $G_n(v) \approx \sum_{k=-1}^{1} G_T(\frac{n-kN}{NT})G_R(\frac{n+v-kN}{NT})$, i.e., with 3 dominant terms only, and $L' = 8$ if not mentioned explicitly. The use of $G_n(v) = E[G_n(v,\zeta)]$ gives almost the same simulation results and hence they are omitted.

Fig. 5 presents the probability of failure of the considered PAEs in the multipath Rayleigh fading channel under perfect timing synchronization and no fractional CFO. We keep the same pilot energy for all the PAEs (i.e., $E_p = 2$). As can be seen, the proposed PAE performs much better than MM's PAE and TS's PAE because their developments correspond to AWGN channel and neglect energy loss information. The proposed PAE also outperforms DT's PAE substantially and the reasons are as follows. The proposed PAE uses knowledge of both the CFO-induced energy loss (to be illustrated in Fig. 6) and limited channel delay spread while DT's PAE neglects those factors. The proposed PAE exploits both magnitude and phase information of the transmitted symbol constellation while DT's PAE only uses the phase information. The CFO-induced energy loss yields a model mismatch for DT's PAE which still remains even if SNR becomes large, causing a performance floor. The performances of the proposed PAE and DT's PAE under sampling offset are also shown in dashed curves; as mentioned in Section IV-A, sampling offset causes additional energy loss on edge tones and degrades performance of both estimators.The proposed PAE is more sensitive to sampling offset, however it still outperforms other estimators even when the sampling offset increases to its maximum possible value 0.5.

In Fig. 6, we show the performance of the proposed PAE using versus ignoring the energy loss information in the accurate signal model under perfect timing synchronization and no fractional CFO. The results clearly show that using the energy loss information improves the proposed PAE's performance. When the CFO value increases, the received filter output signal has more energy loss which will lead to performance degradation. However, if we use the CFO-induced energy loss information as we did in the proposed PAE, we can compensate for the loss substantially. As we can see, when the normalized CFO value changes from 4 to 8, the performance degradation in terms of SNR loss at 10^{-4} failure probability is about 4 dB if energy loss is ignored and only about 1 dB if energy loss is incorporated.

Fig. 7 gives the performance comparison between the proposed PAE and DT's PAE in the presence of different timing and sampling offsets and ICFOs. Comparison between the two sub-

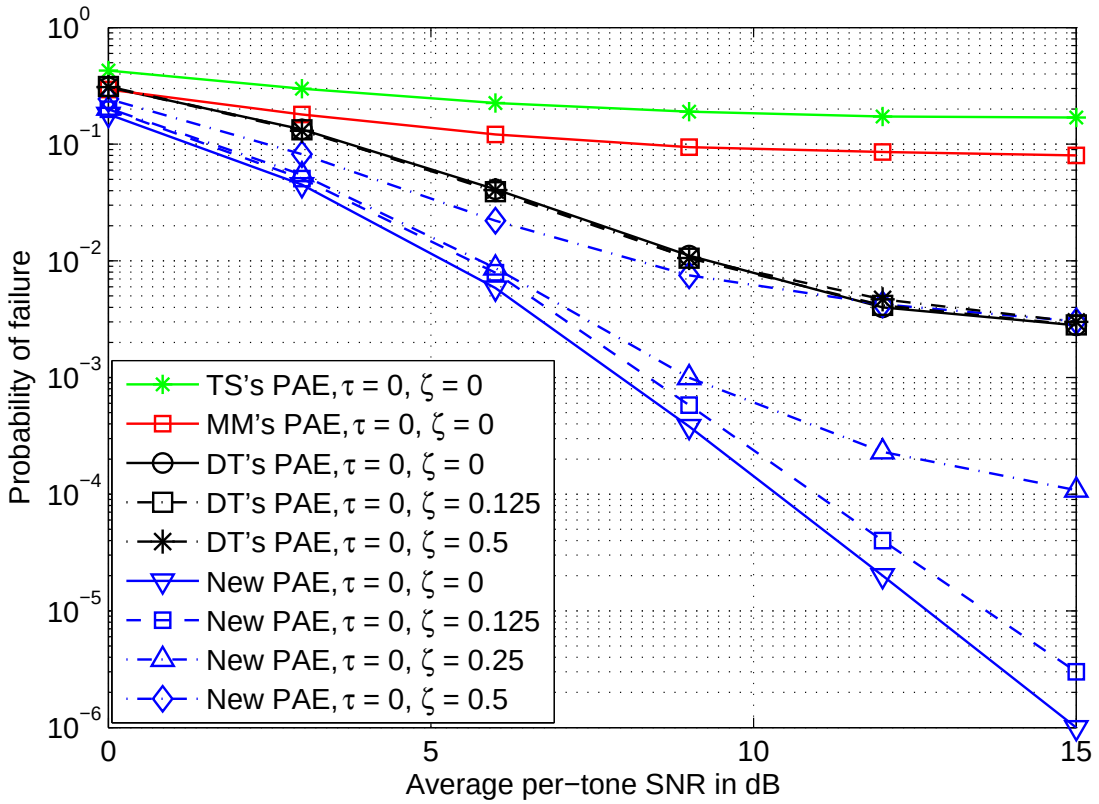

Figure 5. Performance comparison of different ICFO estimators under the accurate signal model with $v = 4$

plots shows that timing offset τ affects the performance of the proposed PAE. The reason is that the proposed PAE uses the knowledge of limited channel delay spread which is affected by both timing and sampling offsets. As mentioned in Section IV-A, the effective channel length L' can be set appropriately to alleviate the impact of timing and sampling offsets. A longer length L' is needed to absorb the effect of timing and sampling offsets in the proposed PAE but it also increases the noise level of the channel estimate. At low SNR where the increased noise level is more dominant than the tail channel taps with very weak energy, $L' = L$ gives better performance. At high SNR where the tail channel taps are more significant than the increased noise level, a longer length $L' = L + \tau$ yields a better result.

Fig. 8 presents the effect of residual fractional CFO on the proposed PAE and DT's PAE under perfect timing synchronization as well as under a more practical scenario with uniformly distributed random timing offset, sampling offset, and CFO ($\tau \in \{1, 2\}$, $\zeta \in [-0.125, 0.125]$, and

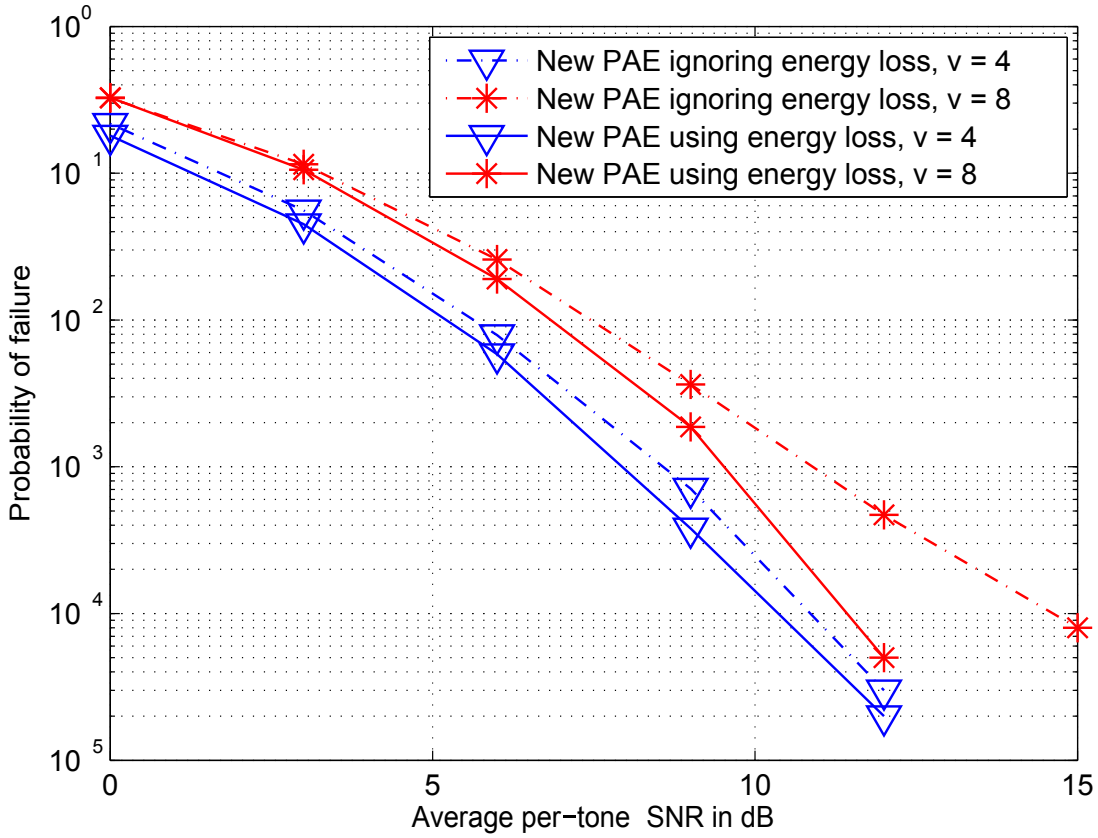

Figure 6. ICFO estimation performances of the new PAE using versus ignoring the energy loss information under the accurate signal model.

$\varepsilon \in [3.5, 4.5]$). The proposed PAE uses $L' = 8$ at low SNR ($\leq 6\text{dB}$) and $L' = 10$ at high SNR ($> 6\text{dB}$). The FCFO estimator in [7] is adopted to compensate for the FCFO. Both methods experience slight performance degradation if compared to the case with perfect fractional CFO compensation. The proposed PAE still exhibits significant gains over DT's PAE.

Fig. 9 shows the performance of the proposed PAE and DT's PAE for several QAM data modulation orders (under $\tau = 0$, uniform $\zeta \in [-0.125, 0.125]$, no residual FCFO). Because DT's PAE assumes PSK constellation, it shows degraded performance in high order QAM systems. However, our proposed PAE performs well in both low and high order QAM systems, with just slight performance degradation for high order QAM at high SNR. Fig. 9 also compares the analytical approximate failure probability of the proposed PAE with the simulation result. At low

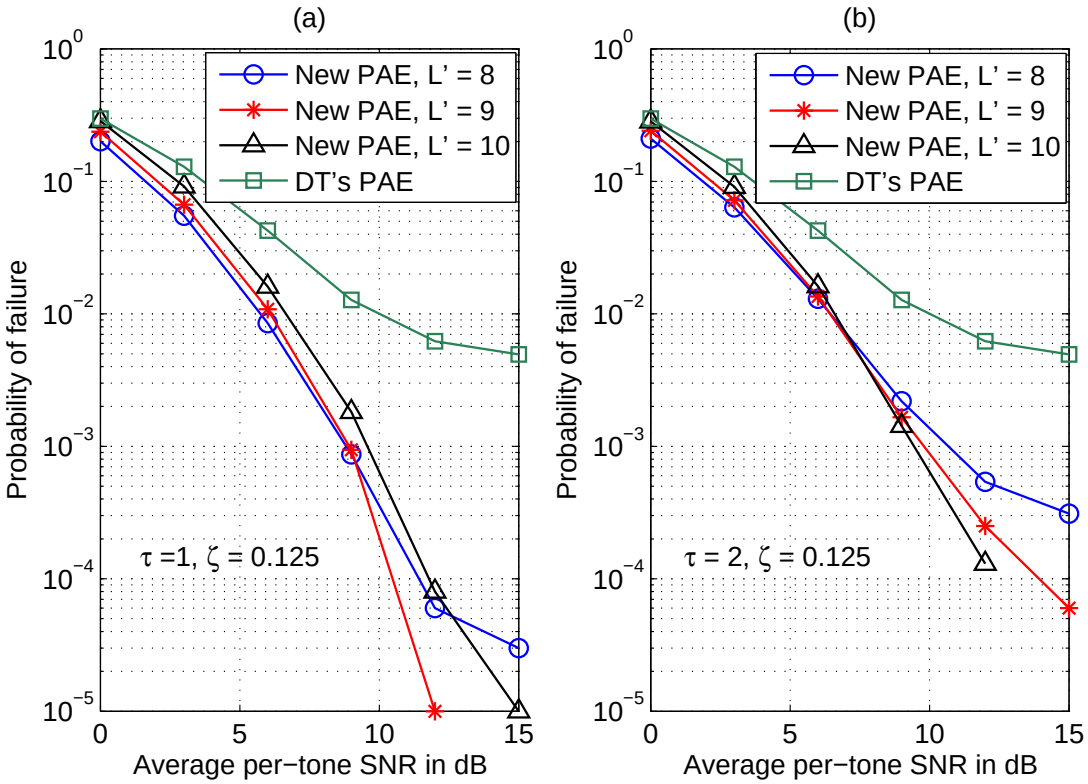

Figure 7. Performance comparison between the proposed PAE and DT's PAE in the presence of timing and sampling offsets at $v = 4$.

SNR (≤ 6dB), (56) and (48) are used to calculate the analytical approximate failure probability. The detection performance of data tones improves as SNR increases, and thus (60) is used at high SNR (> 6dB). We observe that the analytical result is within about 1.5 dB SNR of the simulation result. The performance gap is due to approximation inaccuracy in applying central limit theorem for the distance metric and in the independence assumption between distance metrics in developing the analytical result. As simulation results show that higher order QAM experiences just small performance degradation, the analytical result derived for 4-QAM can still be used as an approximate one for higher order QAM.

Fig. 10 compares the probability of failure of the proposed BE with DT's BE under different ICFO values. Fig. (a) is under perfect timing synchronization and no FCFO. Fig. (b) is for a more practical scenario with uniformly distributed random timing offset, sampling offset, and CFO (same setting as in Fig. 8). The energy loss caused by sampling offset and the inter-carrier

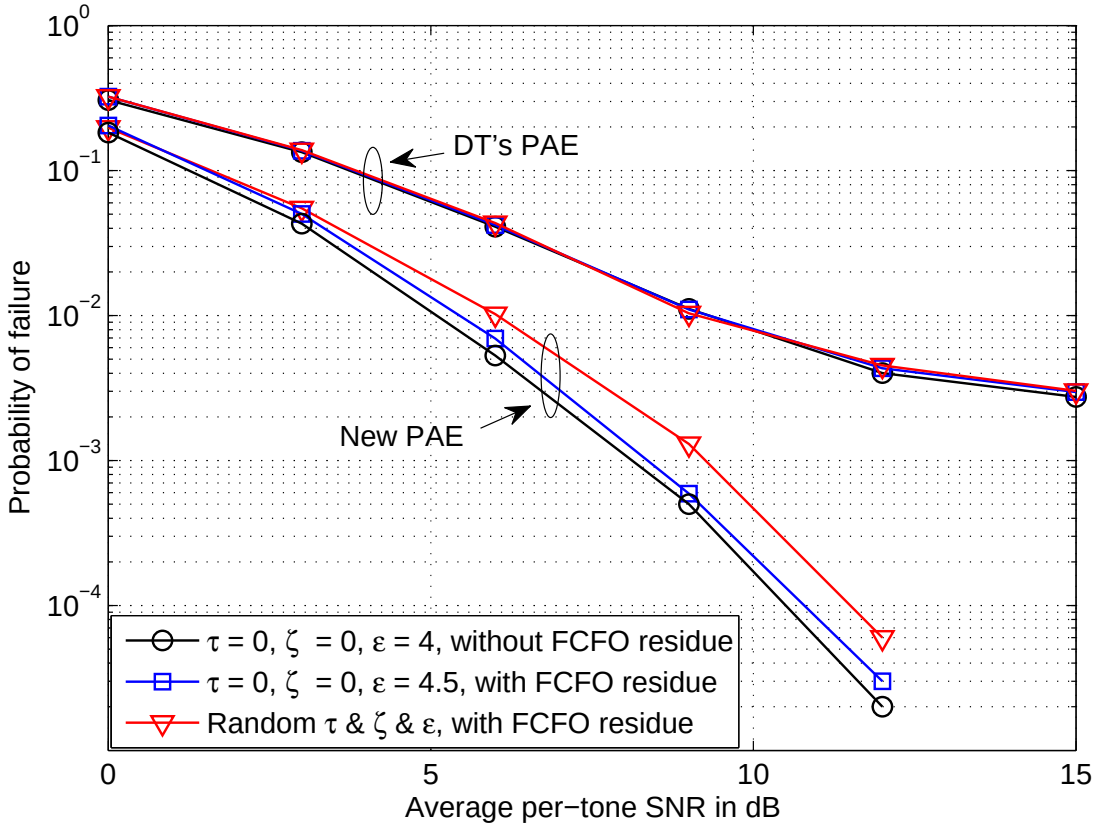

Figure 8. Effect of residual FCFO on ICFO estimation performance of the new PAE and DT's PAE.

interference caused by FCFO degrade performance of both BEs slightly. The performance results with different sampling offsets are almost the same, so we omit the corresponding plots. When the actual ICFO value increases, the performance of DT's BE degrades as we discussed in Section III-B. However, the performance of the proposed BE improves when the actual ICFO value increases. The reason is as follows. A large value of ICFO causes a serious energy loss on some tones and the proposed BE exploits that aspect by regarding those tones as attenuated tones (similar to null tones) in contrast to treating them as unknown data tones as in the existing BEs. In blind estimation of CFO, null tones play a similar role as pilots in PAE. Thus, the performance advantage of the proposed BE over the existing BEs is more pronounced at larger ICFO values.

Fig. 11 shows the effects of QAM data modulation order on the performance of the proposed

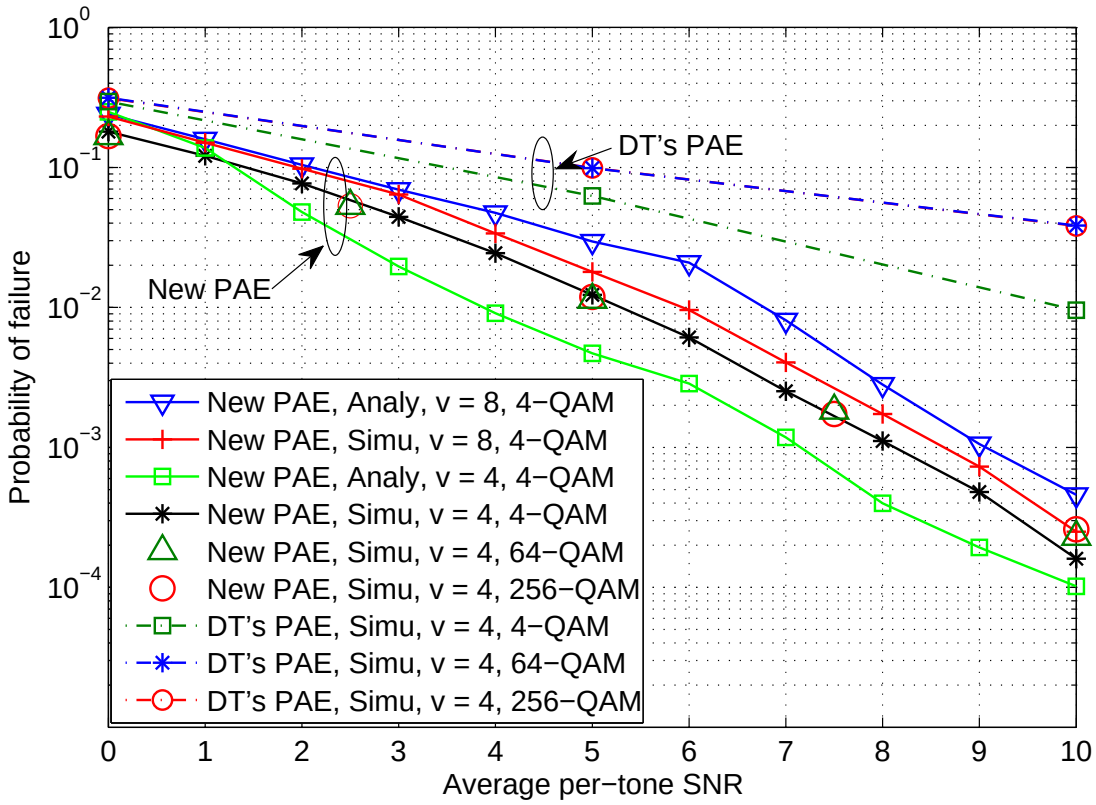

Figure 9. Effects of QAM order on the performance of the new PAE and DT's PAE, and comparison between the simulation and approximate analytical results of the new PAE ($\tau = 0$, uniform random $\zeta \in [-0.125, 0.125]$).

BE and DT's BE (under $\tau = 0$, uniform $\zeta \in [-0.125, 0.125]$, no residual FCFO). Because DT's BE assumes PSK modulation, it fails in high order QAM systems. However, our proposed BE maintains similar performance in both low and high order QAM systems with just slight degradation for high order QAM. Fig. 11 also compares the analytical approximate failure probability of the proposed BE with the simulation result. The analytical result for the proposed BE holds for different QAM orders and it shows a close match with the simulation result for 4-QAM and slight degradation in accuracy for high order QAM at high SNR. This is due to the Gaussian assumption of the received signal in the derivation which is accurate for 4-QAM but an approximation for high order QAM.

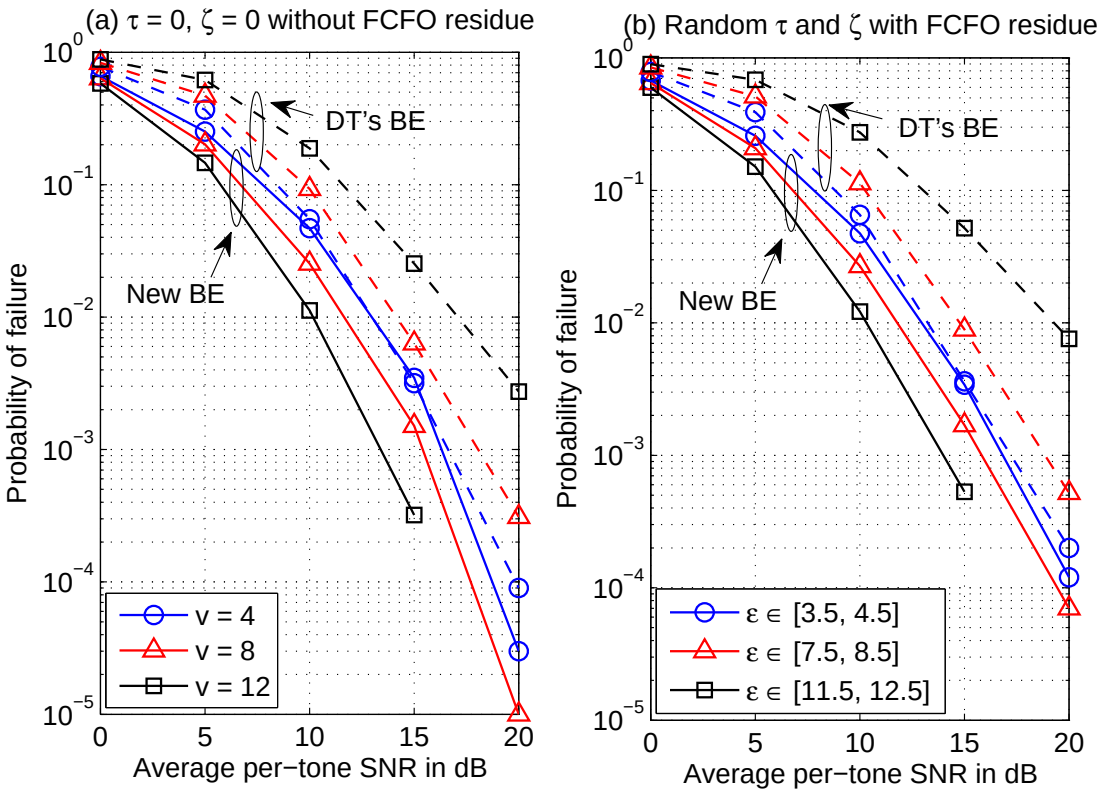

Figure 10. Effects of different CFO values on the estimation performances of the new BE and DT's BE

C. Complexity Comparison of the ICFO Estimators

Table II presents the complexities of the considered PAE and BE estimators. For the system setting as in the simulation, for each value of $\tilde{v}$, the proposed PAE requires 6063 operations while DT's, MM's, and TS's PAEs need 995, 1024, and 225 operations; the proposed BE requires 374 operations while DT's, MM's and TS's BEs need 895, 447 and 1568 operations, respectively. Note that the proposed PAE has higher complexity than the others (but at the same $O(n)$ level except TS's PAE) but it also provides channel estimates in addition to better ICFO estimates. The proposed BE achieves the complexity reduction and performance improvement at the same time, if compared to the reference methods. Furthermore, both of the proposed methods can be applied with a broader class of modulation schemes than the reference methods.

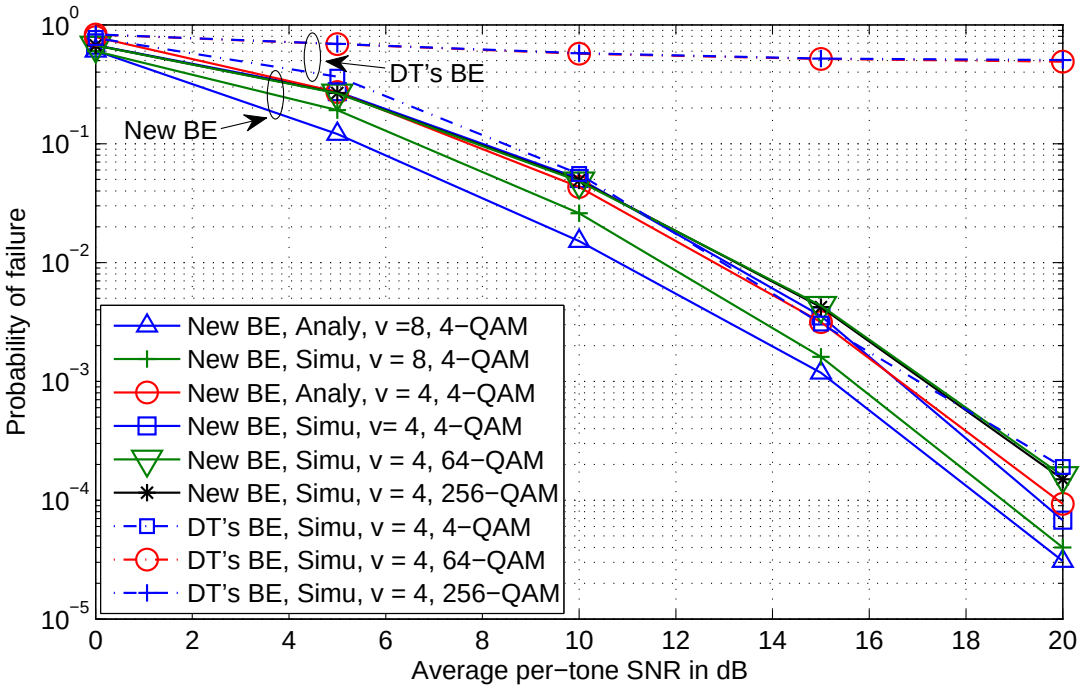

Figure 11. Effects of QAM order on the performance of the new BE and DT's BE, and comparison between the simulation and approximate analytical results of the new BE ($\tau = 0$, uniform random $\zeta \in [-0.125, 0.125]$).

VII. Conclusions

This paper presents an accurate signal model for OFDM systems with a receiver matched filter in the presence of CFO, timing offset and sampling offset, and based on this model this paper investigates the effects of these offsets on CFO estimation. CFO causes signal distortion and band-edge energy loss while sampling offset yields additional band-edge energy loss and channel energy leakage to adjacent channel taps. Our investigations show that correlation-based estimators are only affected by the energy loss due to CFO and sampling offset while maximum likelihood based estimators or their variants which are developed under the commonly used signal model deviate from their optimality due to all of the above factors. We have also discussed pilot design conditions to avoid or lessen the band-edge energy loss. Furthermore, we have developed new pilot-aided and blind integer normalized CFO estimators based on the accurate signal model and introduced distinctively spaced null tones in blind estimation. We have also illustrated that in the presence of timing and sampling offsets, the effective channel has a longer length (in delay

Table II

COMPLEXITY OF ESTIMATORS AT EACH CANDIDATE ICFO VALUE

Algorithm	Real products	Real additions
New PAE	$(4L+12)N$ $+(4L-6)S-6V$	$(4L+6)N+(4L-2)S$ $-2V-2L-1$
DT's PAE	$4(2N-V+1)$	$8N-2S-6V-1$
MM's PAE	$4(2N+S-V)$	$6N+4S-4V$
TS's PAE	$8S+2$	$6S-1$
New BE	$3N$	$3N-V-2$
DT's BE	$8(N-V)$	$8(N-V)-1$
MM's BE	$4(N-V)$	$4(N-V)-1$
TS's BE	$18(N-V)$	$10(N-V)$

domain) and hence any channel estimator which exploits the limited channel delay would need to incorporate this, especially at high SNR. Analytical approximate failure probability expressions for integer normalized CFO estimation of the proposed pilot-aided and blind estimators are also presented. Simulation results corroborate that the proposed estimators have broader applicability (to both PSK and QAM) and better estimation performance than the existing ones.

APPENDIX A

Here, we prove the Proposition in Section V-A. We have $E\left[d_k^*(\tilde{v})d_{k+l}(\tilde{v})\right] = E\big[(R_k-\hat{R}_k(\tilde{v}))^*(R_{k+l}-\hat{R}_{k+l}(\tilde{v}))\big] = 0$ for $l \neq 0$, due to zero-mean independent $\{a_{k-\tilde{v}}\}$. Then, with $d_k(\tilde{v}) \sim \mathcal{CN}(0, V_k(\tilde{v}))$, we have independent $\{d_k(\tilde{v})\}$ for different k, and by the central limit theorem, we can approximate $\mathcal{M}(\tilde{v})$ as Gaussian. The covariance matrix $\boldsymbol{V}(\tilde{v})$ of $\mathbf{d}(\tilde{v})$ is a diagonal matrix with diagonal elements $\{V_k(\tilde{v})\}$. From $\mathbf{d}(\tilde{v}) \sim \mathcal{CN}(0, \boldsymbol{V}(\tilde{v}))$, we obtain that $\mathcal{M}(\tilde{v})$ has the mean $u_{\mathcal{M}}(\tilde{v}) = \mathrm{Tr}(\boldsymbol{V}(\tilde{v})) = \sum_k V_k(\tilde{v})$ and variance $\sigma^2_{\mathcal{M}}(\tilde{v}) = \mathrm{Tr}(\boldsymbol{V}(\tilde{v})^2) = \sum_k V_k^2(\tilde{v})$. Thus, the pdf of $\mathcal{M}(\tilde{v})$ is $f_{\mathcal{M}}(\tilde{v}) = \mathcal{N}(u_{\mathcal{M}}(\tilde{v}), \sigma^2_{\mathcal{M}}(\tilde{v}))$. For $\tilde{v} \neq v$, the pair-wise probability of failure (giving a wrong ICFO estimate) can be calculated as:

$$P\big(\mathcal{M}(v) > \mathcal{M}(\tilde{v})\big) = \int_{-\infty}^{\infty} f_{\mathcal{M}(v)}(t)\left(\int_{-\infty}^{t} f_{\mathcal{M}(\tilde{v})}(u)du\right)dt$$
$$\approx \int_{-\infty}^{\infty} f_{\mathcal{M}(v)}(t)\left(1-\mathrm{Q}(\frac{t-u_{\mathcal{M}}(\tilde{v})}{\sigma_{\mathcal{M}}(\tilde{v})})\right)dt. \quad (53)$$

Using the fact that $E\left[\mathrm{Q}(u+\lambda x)\right]=\mathrm{Q}\left(\frac{u}{\sqrt{1+\lambda^2}}\right)$ for $x\sim\mathcal{N}(0,1)$ [25], we can simplify (53) as

$$P\left(\mathcal{M}(v)>\mathcal{M}(\tilde{v})\right)\approx 1-\mathrm{Q}\left(\frac{u_{\mathcal{M}}(v)-u_{\mathcal{M}}(\tilde{v})}{\sigma_{\mathcal{M}}(\tilde{v})\sqrt{1+\sigma^2_{\mathcal{M}}(v)/\sigma^2_{\mathcal{M}}(\tilde{v})}}\right). \tag{54}$$

For a different candidate CFO $\tilde{v}$, a different set of received tones will be used to estimate the channel, so we can assume the estimated symbols on the kth tone $\hat{R}_k(\tilde{v})$ for different values of candidate ICFO $\tilde{v}$ are independent. Then the metric values for different values of candidate CFO $\tilde{v}$ can also be approximated as independent. Then we have

$$P_{\text{PAE fail}}\approx 1-\prod_{\tilde{v}\neq v}\left(1-P\left(\mathcal{M}(v)>\mathcal{M}(\tilde{v})\right)\right). \tag{55}$$

This completes the proof.

In the following, $V_k(\tilde{v})$ is computed. We have

$$V_k(\tilde{v})=E\left[|R_k-\hat{R}_k(\tilde{v})|^2\right]=E\left[|R_k|^2-2\Re\left\{R_k\hat{R}^*_k(\tilde{v})\right\}+\left|\hat{R}_k(\tilde{v})\right|^2\right] \tag{56}$$

where $E\left[|R_k|^2\right]=G^2_{k-v}(v)E[|a_{k-v}|^2]+\sigma^2$. In systems with boosted pilots, $E[|a_k|^2]=E_p>1$ when $k\in\mathcal{P}$ and $E[|a_k|^2]=1$ when $k\in\mathcal{D}$.

The third item in (56) can be written as

$$\begin{aligned}E\left[|\hat{R}_k(\tilde{v})|^2\right]&=G^2_{k-\tilde{v}}(\tilde{v})E\left[|\mathbf{y}^H_{k-\tilde{v}}(\tilde{v})\mathbf{A}^H_p\mathbf{R}_p(\tilde{v})\hat{a}_{k-\tilde{v}}(\tilde{v})|^2\right]\\&=E\left[|\hat{a}_{k-\tilde{v}}(\tilde{v})|^2\right]E_pG^2_{k-\tilde{v}}(\tilde{v})\mathbf{y}^H_{k-\tilde{v}}(\tilde{v})E\left[\mathbf{R}_p(\tilde{v})\mathbf{R}^H_p(\tilde{v})\right]\mathbf{y}_{k-\tilde{v}}(\tilde{v}).\end{aligned} \tag{57}$$

When received data tones are mistaken as pilot tones for a candidate ICFO $\tilde{v}$, $E\left[\mathbf{R}_p(\tilde{v})\mathbf{R}^H_p(\tilde{v})\right]=\mathbf{G}^2_{p+\tilde{v}}(v)+\sigma^2\mathbf{I}$. When a candidate CFO $\tilde{v}$ corresponds to the scenario with the correct receive pilot tones set but with a wrong order due to a cyclic shift (it occurs when cyclically equi-spaced pilots are used), $E\left[\mathbf{R}_p(\tilde{v})\mathbf{R}^H_p(\tilde{v})\right]=E_p\mathbf{G}^2_{p+\tilde{v}}(v)+\sigma^2\mathbf{I}$. For $k\in\mathcal{D}$, we have $E[|\hat{a}_k(\tilde{v})|^2]=1$. For $k\in\mathcal{P}$, we have $\hat{a}_k(\tilde{v})=a_k$ and $E[|\hat{a}_k(\tilde{v})|^2]=E_p$.

In the performance analysis for PAE, we only consider 4-QAM. Since $\tilde{a}_k(\tilde{v})$ for $k\in\mathcal{D}$ is mapped to $\hat{a}_k(\tilde{v})$ by means of the nearest modulation constellation point, the phase difference between $\tilde{a}_k(\tilde{v})$ and $\hat{a}_k(\tilde{v})$ is always within the range $[-\frac{\pi}{4},\frac{\pi}{4})$ for 4-QAM when $k\in\mathcal{D}$. Since $R_{k+\tilde{v}}=\tilde{a}_k(\tilde{v})\hat{H}_k(\tilde{v})G_k(\tilde{v})$ from (40) and $\hat{R}_{k+\tilde{v}}(\tilde{v})=\hat{a}_k(\tilde{v})\hat{H}_k(\tilde{v})G_k(\tilde{v})$, the phase difference between R_k and $\hat{R}_k$ on a data tone is also always within the range $[-\frac{\pi}{4},\frac{\pi}{4})$ for 4-QAM. When $\tilde{v}\neq v$, the received tones used in the pilot-based channel estimation correspond to random data instead of pilots, and hence the phase of $\tilde{a}_k(\tilde{v})$ is uniformly distributed in $[-\pi,\pi)$ while

the phase difference between $\tilde{a}_k(\tilde{v})$ and $\hat{a}_k(\tilde{v})$ is uniformly distributed within $[-\frac{\pi}{4}, \frac{\pi}{4})$. Then the phase difference between $\hat{R}_k(\tilde{v})$ and R_k is also uniformly distributed within $[-\frac{\pi}{4}, \frac{\pi}{4})$. Since $|\hat{a}_k(\tilde{v})| = 1$, $|\tilde{a}_k(\tilde{v})|$ is independent of $|\hat{a}_k(\tilde{v})|$ and $|R_k|$ is independent of $|\hat{R}_k(\tilde{v})|$. Then, the second item in (56) becomes

$$E\left[2\Re\left\{R_k\hat{R}_k^*(\tilde{v})\right\}\right] = \frac{8}{\pi}\int_0^{\frac{\pi}{4}} E\big[|R_k|\big]\cdot E\big[|\hat{R}_k(\tilde{v})|\big]\cos\theta \; d\theta, \text{ for } k-\tilde{v}\in\mathcal{D} \text{ and } \tilde{v}\neq v, \quad (58)$$

where $|R_k|$ and $|\hat{R}_k(\tilde{v})|$ are independent Rayleigh random variables with $E\big[|R_k|\big] = \frac{1}{2}\sqrt{\pi E\big[|R_k|^2\big]}$ and $E|\hat{R}_k(\tilde{v})| = \frac{1}{2}\sqrt{\pi E\big[|\hat{R}_k(\tilde{v})|^2\big]}$. If $k-\tilde{v} = p_i \in \mathcal{P}$, (58) dose not hold because $\hat{a}_{k-\tilde{v}}$ is given by the known pilot a_{p_i} and no detection is performed on this tone. In this case, we can compute the second term in (56) by

$$\begin{aligned} E\left[\Re\left\{R_k\hat{R}_k^*(\tilde{v})\right\}\right] =& \Re\left\{E_pG_{k-\tilde{v}}(\tilde{v})\mathbf{e}_i^H\mathbf{y}_{k-\tilde{v}}(\tilde{v})E[|R_k|^2]\right\} \\ =& \Re\left\{E_pG_{k-\tilde{v}}(\tilde{v})\mathbf{e}_i^H\mathbf{y}_{k-\tilde{v}}(\tilde{v})\left(G_{k-v}^2(v)E[|a_{k-v}|^2]+\sigma^2\right)\right\} \end{aligned} \quad (59)$$

where $\mathbf{e}_i$ is an $N\times 1$ vector of which the ith element is 1 and all the others are zeros.

If $\tilde{v} = v$, we have $\hat{H}_k(v) = H_k + \mathbf{y}_k^H(v)\mathbf{A}_p^H\mathbf{Z}_p(v)$, and together with an assumption of $\hat{a}_k(v) = a_k$ at high SNR, we can represent $V_k(v)$ as

$$\begin{aligned} V_k(v) =& E\left[|R_k-\hat{R}_k(v)|^2\right] = E\left[|a_{k-v}G_{k-v}(v)H_{k-v} + Z_k - \hat{H}_k(v)G_{k-v}(v)\hat{a}_{k-v}(v)|^2\right] \quad (60)\\ =& E\left[|Z_k - \mathbf{y}_k^H(v)\mathbf{A}_p^H\mathbf{Z}_p(v)G_{k-v}(v)\hat{a}_{k-v}(v)|^2\right] \\ =& E\left[|Z_k|^2 - 2\Re\left\{Z_k\hat{a}_{k-v}^*(v)G_{k-v}(v)\mathbf{Z}_p^H(v)\mathbf{A}_p\mathbf{y}_k(v)\right\}\right] \\ &+ \sigma^2E\left[|\hat{a}_{k-v}(v)|^2\right]E_pG_{k-v}^2(v)\mathbf{y}_{k-v}^H(v)\mathbf{y}_{k-v}(v). \end{aligned}$$

If $k-v\in\mathcal{D}$, we have $E\left[|\hat{a}_{k-v}(v)|^2\right] = 1$ and Z_k is independent of $\mathbf{Z}_p(v)$, which yields $E\left[2\Re\left\{Z_k\hat{a}_k^*(v)G_{k-v}(v)\mathbf{Z}_p^H(v)\mathbf{A}_p\mathbf{y}_k(v)\right\}\right] = 0$. If $k-v = p_i\in\mathcal{P}$, $\hat{a}_{k-v}(v) = a_{k-v}(v)$ which is independent of Z_k and $\mathbf{Z}_p(v)$, and we have $E\left[2\Re\left\{Z_k\hat{a}_k^*(v)G_{k-v}(v)\mathbf{Z}_p^H(v)\mathbf{A}_p\mathbf{y}_k(v)\right\}\right] = 2\sigma^2E_p\Re\left\{\boldsymbol{e}_i^H\mathbf{y}_k(v)G_{k-v}^H(v)\right\}$. We use (56) to approximate the variance of the distance square metric on data tones at low SNR (as the data detection results are not so reliable) and (60) at high SNR (due to reliable data detection results).

APPENDIX B

Proof for Proposition in Section V-B is given below. Define $\hat{\mathbf{q}}(\tilde{v}) = \mathbf{U}(\tilde{v})\bar{\mathbf{q}}$. Then we can express (49) as

$$\begin{aligned}\Lambda(\tilde{v}) - \Lambda(v) &= \hat{\mathbf{q}}^H(\tilde{v})\mathbf{\Sigma}(\tilde{v})\hat{\mathbf{q}}(\tilde{v}) + c(\tilde{v}) \\ &= \alpha_1 - \alpha_2 + c(\tilde{v}) \end{aligned} \tag{61}$$

where $\alpha_1 = \sum_{i=1}^{n_{\tilde{v}}^+} \lambda_i^+(\tilde{v})|\hat{q}(\tilde{v},i)|^2$, $\alpha_2 = -\sum_{i=1}^{n_{\tilde{v}}^-} \lambda_i^-(\tilde{v})|\hat{q}(\tilde{v},i)|^2$, and $\hat{q}(\tilde{v},i)$ is the ith element of $\hat{\mathbf{q}}(\tilde{v})$. Since $\hat{\mathbf{q}} \sim \mathcal{CN}(0,\mathbf{I})$, α_1 and α_2 are independent and their pdfs can be obtained from [26] as

$$f_{\alpha_1}(x) = \sum_{i=1}^{n_{\tilde{v}}^+} \varsigma_i^+(\tilde{v}) e^{-\frac{x}{\lambda_i^+(\tilde{v})}}, \ x > 0, \tag{62}$$

$$f_{\alpha_2}(x) = \sum_{i=1}^{n_{\tilde{v}}^-} \varsigma_i^-(\tilde{v}) e^{-\frac{x}{\lambda_i^-(\tilde{v})}}, \ x > 0, \tag{63}$$

where $\varsigma_i^+(\tilde{v}) = \frac{1}{\lambda_i^+(\tilde{v})} \prod_{k=1,k\neq i}^{n_{\tilde{v}}^+} (\frac{\lambda_i^+(\tilde{v})}{\lambda_i^+(\tilde{v})-\lambda_k^+(\tilde{v})})$ and $\varsigma_i^-(\tilde{v}) = \frac{1}{\lambda_i^-(\tilde{v})} \prod_{k=1,k\neq i}^{n_{\tilde{v}}^-} (\frac{\lambda_i^-(\tilde{v})}{\lambda_i^-(\tilde{v})-\lambda_k^-(\tilde{v})})$. Then a straight computation from (61), (62), and (63) yields $P[\Lambda(\tilde{v}) > \Lambda(v)]$ as in (52).

Next, we know that

$$P\big[E_{1,2}\big] \approx \begin{cases} P_1 P_2, & \rho_1 = 0 \\ \min(P_1, P_2), & \rho_1 = 1. \end{cases} \tag{64}$$

The proposed BE uses a set of distinctively spaced null tones and its feature is that $\Lambda(\tilde{v}_i)$, $\tilde{v}_i \neq v$, contains similar small number of overlaps between the received null tones set and a trial null tones set for adjacent values of i. Thus, the difference between P_i and P_{i+1} is small, e.g., $\min(P_1, P_2) \approx P_1$. Based on (64) which gives probabilities at two end points of ρ_1, we can approximate the probability at an intermediate point of ρ_1 as a quadratic interpolation in the form $a\rho_1^2 + b$ which yields

$$P\big[E_{1,2}\big] \approx P_1 \left(\rho_1^2(1 - P_2) + P_2\right), \ 0 < \rho_1 < 1. \tag{65}$$

Next, we have

$$P\big[E_{1,2,3}\big] = P\big[E_{1,2}\big] P\big[E_3 | E_{1,2}\big]. \tag{66}$$

Since $\Lambda(\tilde{v}_3)$ is more correlated with $\Lambda(\tilde{v}_2)$ than $\Lambda(\tilde{v}_1)$, we can approximate that

$$P\big[E_3 | E_{1,2}\big] \approx \rho_2^2(1 - P_3) + P_3, \tag{67}$$

and substituting (67) into (66) we obtain

$$P\left[E_{1,2,3}\right] \approx P_1 \left(\rho_1^2(1-P_2)+P_2\right)\left(\rho_2^2(1-P_3)+P_3\right). \tag{68}$$

Thus, we can deduce that the estimation success probability of the proposed BE is

$$P_{\text{BE success}} = P\left[E_{1,2,\cdots,K}\right] \approx P_1 \prod_{i=2}^{K}(\rho_{i-1}^2(1-P_i)+P_i) \tag{69}$$

which completes the proof.

APPENDIX C

For the performance analysis of the proposed BE, the correlation coefficient between $\Lambda(\tilde{v}_i)$ and $\Lambda(\tilde{v}_{i+1})$ can be computed as

$$\rho_i = \frac{E\left[(\hat{\Lambda}(\tilde{v}_i)-E[\hat{\Lambda}(\tilde{v}_i)])(\hat{\Lambda}(\tilde{v}_{i+1})-E[\hat{\Lambda}(\tilde{v}_{i+1})])\right]}{\sigma_{\hat{\Lambda}}(\tilde{v}_i)\sigma_{\hat{\Lambda}}(\tilde{v}_{i+1})} \tag{70}$$

where

$$\hat{\Lambda}(\tilde{v}_i) = \left[\mathbf{A}(v)\mathbf{G}(v)\mathbf{F}_L\mathbf{h}+\mathbf{Z}\right]^H \hat{\mathbf{\Upsilon}}(\tilde{v}_i)\left[\mathbf{A}(v)\mathbf{G}(v)\mathbf{F}_L\mathbf{h}+\mathbf{Z}\right], \tag{71}$$

$$\hat{\Upsilon}_k(\tilde{v}_i) = \begin{cases} \frac{1}{G_{k-\tilde{v}_i}^2(\tilde{v}_i)+\sigma^2}, & k-\tilde{v}_i \in \mathcal{D} \\ \frac{1}{\sigma^2}, & k-\tilde{v}_i \in \mathcal{V}, \end{cases} \tag{72}$$

$$\sigma_{\hat{\Lambda}}(\tilde{v}_i) = \sqrt{E[\hat{\Lambda}^2(\tilde{v}_i)]-E[\hat{\Lambda}(\tilde{v}_i)]^2}. \tag{73}$$

We know that $\mathbf{A}(v)\mathbf{A}^H(v) = \mathbf{I}'(v)$ where $\mathbf{I}'(v)$ is an $N \times N$ diagonal matrix with the ith diagonal element being equal to 1 for $i-v \in \mathcal{D}$ and 0 for $i-v \in \mathcal{V}$. Denote $\mathbf{\Psi}_{\tilde{v}_i} = \mathbf{F}_L^H\mathbf{G}^H(v)\mathbf{I}'(v)\hat{\mathbf{\Upsilon}}(\tilde{v}_i)\mathbf{G}(v)\mathbf{F}_L$ and $\psi_{\tilde{v}_i}(l,j)$ as its lth row jth column element. Then we have

$$E[\hat{\Lambda}(\tilde{v}_i)] = \text{Tr}(\mathbf{C_h}\mathbf{\Psi}_{\tilde{v}_i}) + \text{Tr}(\hat{\mathbf{\Upsilon}}(\tilde{v}_i))\sigma^2, \tag{74}$$

$$E[\hat{\Lambda}^2(\tilde{v}_i)] = V_1 + 2V_2 + 2V_3 + V_4 \tag{75}$$

where $V_1 = E[\mathbf{h}^H\mathbf{\Psi}_{\tilde{v}_i}\mathbf{h}\mathbf{h}^H\mathbf{\Psi}_{\tilde{v}_i}\mathbf{h}]$, $V_2 = E[\mathbf{h}^H\mathbf{\Psi}_{\tilde{v}_i}\mathbf{h}\mathbf{Z}^H\hat{\mathbf{\Upsilon}}(\tilde{v}_i)\mathbf{Z}]$, $V_3 = E[\mathbf{h}^H\mathbf{F}_L^H\mathbf{G}^H(v)\mathbf{A}^H(v)\hat{\mathbf{\Upsilon}}(\tilde{v}_i)\ \mathbf{Z}\mathbf{Z}^H\hat{\mathbf{\Upsilon}}(\tilde{v}_i)\mathbf{A}(v)\mathbf{G}(v)\mathbf{F}_L\mathbf{h}]$, and $V_4 = E[\mathbf{Z}^H\hat{\mathbf{\Upsilon}}(\tilde{v}_i)\mathbf{Z}\mathbf{Z}^H\hat{\mathbf{\Upsilon}}(\tilde{v}_i)\mathbf{Z}]$. For a uncorrelated multipath Rayleigh fading channel with the power delay profile of $\{\sigma_{h_l}^2\}$, we have

$$V_1 = \sum_{l=1}^{L}\sum_{j=1,j\neq l}^{L}\left[\psi_{\tilde{v}_i}(l,l)\psi_{\tilde{v}_i}(j,j)+\psi_{\tilde{v}_i}(l,j)\psi_{\tilde{v}_i}(j,l)\right]$$

$$\cdot \sigma_{h_l}^2\sigma_{h_j}^2 + 2\sum_{l=1}^{L}\psi_{\tilde{v}_i}^2(l,l)\sigma_{h_l}^4, \tag{76}$$

$$V_2 = \mathrm{Tr}(\mathbf{C_h}\mathbf{\Psi}_{\tilde{v}_i})\mathrm{Tr}(\hat{\mathbf{\Upsilon}}(\tilde{v}_i))\sigma^2, \tag{77}$$

$$V_3 = \mathrm{Tr}\left(\mathbf{C_h}\mathbf{F}_L^H\mathbf{G}^H(v)\mathbf{I}'(v)\hat{\mathbf{\Upsilon}}^2(\tilde{v}_i)\mathbf{G}(v)\mathbf{F}_L\right)\sigma^2, \tag{78}$$

$$V_4 = \left(\mathrm{Tr}(\hat{\mathbf{\Upsilon}}(\tilde{v}_i))\mathrm{Tr}(\hat{\mathbf{\Upsilon}}(\tilde{v}_i)) + \mathrm{Tr}(\hat{\mathbf{\Upsilon}}^2(\tilde{v}_i))\right)\sigma^4. \tag{79}$$

Similarly, we have

$$\begin{aligned}
E\left[\hat{\Lambda}(\tilde{v}_i)\hat{\Lambda}(\tilde{v}_{i+1})\right] &= 2\sum_{l=1}^{V}\psi_{\tilde{v}_i}(l,l)\psi_{\tilde{v}_{i+1}}(l,l)\sigma_{h_l}^4 \\
&+ \sum_{l=1}^{V}\sum_{j=1,j\neq l}^{V}\left[\psi_{\tilde{v}_i}(l,l)\psi_{\tilde{v}_{i+1}}(j,j) + \psi_{\tilde{v}_i}(l,j)\psi_{\tilde{v}_{i+1}}(j,l)\right] \\
&\cdot \sigma_{h_l}^2\sigma_{h_j}^2 + \mathrm{Tr}(\mathbf{C_h}\mathbf{\Psi}_{\tilde{v}_{i+1}})\mathrm{Tr}(\hat{\mathbf{\Upsilon}}(\tilde{v}_{i+1}))\sigma^2 \\
&+ 2\mathrm{Tr}\left(\mathbf{C_h}\mathbf{F}_L^H\mathbf{G}^H(v)\mathbf{I}'(v)\hat{\mathbf{\Upsilon}}(\tilde{v}_i)\hat{\mathbf{\Upsilon}}(\tilde{v}_{i+1})\mathbf{G}(v)\mathbf{F}_L\right)\sigma^2 \\
&+ \left(\mathrm{Tr}(\hat{\mathbf{\Upsilon}}(\tilde{v}_i))\mathrm{Tr}(\hat{\mathbf{\Upsilon}}(\tilde{v}_{i+1})) + \mathrm{Tr}(\hat{\mathbf{\Upsilon}}(\tilde{v}_i)\hat{\mathbf{\Upsilon}}(\tilde{v}_{i+1}))\right)\sigma^4 \\
&+ \mathrm{Tr}(\mathbf{C_h}\mathbf{\Psi}_{\tilde{v}_i})\mathrm{Tr}(\hat{\mathbf{\Upsilon}}(\tilde{v}_i))\sigma^2.
\end{aligned} \tag{80}$$

Substituting (80) and (75) into (70), we obtain ρ_i.

REFERENCES

[1] P. Moose, "A technique for orthogonal frequency division multiplexing frequency offset correction," *IEEE Trans. Commun.*, vol. 42, no. 10, pp. 2908 –2914, Oct. 1994.

[2] T. Pollet, M. Van Bladel, and M. Moeneclaey, "BER sensitivity of OFDM systems to carrier frequency offset and wiener phase noise," *IEEE Trans. Commun.*, vol. 43, no. 234, pp. 191 –193, Feb./Mar./Apr. 1995.

[3] H. Minn, P. Tarasak, and V. Bhargava, "OFDM frequency offset estimation based on BLUE principle," in *Proc. IEEE VTC (Fall)*, vol. 2, 2002, pp. 1230 – 1234.

[4] ——, "Some issues of complexity and training symbol design for OFDM frequency offset estimation methods based on BLUE principle," in *Proc. IEEE VTC (Spring)*, vol. 2, Apr. 2003, pp. 1288 – 1292.

[5] M. Morelli and U. Mengali, "Carrier-frequency estimation for transmissions over selective channels," *IEEE Trans. Commun.*, vol. 48, no. 9, pp. 1580 –1589, Sep. 2000.

[6] M. Morelli and M. Moretti, "Integer frequency offset recovery in OFDM transmissions over selective channels," *IEEE Trans. Wireless Commun.*, vol. 7, no. 12, pp. 5220 –5226, Dec. 2008.

[7] T. Schmidl and D. Cox, "Robust frequency and timing synchronization for OFDM," *IEEE Trans. Commun.*, vol. 45, no. 12, pp. 1613 –1621, Dec. 1997.

[8] M. Morelli, A. D'Andrea, and U. Mengali, "Frequency ambiguity resolution in OFDM systems," *IEEE Commun. Lett.*, vol. 4, no. 4, pp. 134 –136, Apr. 2000.

[9] J. Lei and T.-S. Ng, "A consistent OFDM carrier frequency offset estimator based on distinctively spaced pilot tones," *IEEE Trans. Wireless Commun.*, vol. 3, no. 2, pp. 588 – 599, Mar. 2004.

[10] Y. Li, H. Minn, N. Al-Dhahir, and A. R. Calderbank, "Pilot designs for consistent frequency-offset estimation in OFDM systems," *IEEE Trans. Commun.*, vol. 55, no. 5, pp. 864 –877, May 2007.

[11] H. Minn, X. Fu, and V. Bhargava, "Optimal periodic training signal for frequency offset estimation in frequency-selective fading channels," *IEEE Trans. Commun.*, vol. 54, no. 6, pp. 1081 –1096, Jun. 2006.

[12] N. Noels, H. Steendam, and M. Moeneclaey, "The true cramer-rao bound for carrier frequency estimation from a PSK signal," *IEEE Trans. Commun.*, vol. 52, no. 5, pp. 834 – 844, May 2004.

[13] B. Xie, W. Qiu, and H. Minn, "Exact signal model and new carrier frequency offset compensation scheme for OFDM," *IEEE Trans. Wireless Commun.*, vol. 11, no. 2, pp. 550 –555, Feb. 2012.

[14] O. Salim, A. Nasir, H. Mehrpouyan, W. Xiang, S. Durrani, and R. Kennedy, "Channel, phase noise, and frequency offset in OFDM systems: Joint estimation, data detection, and hybrid cramer-rao lower bound," *IEEE Trans. Commun.*, vol. 62, no. 9, pp. 3311–3325, Sep. 2014.

[15] H. Yang, W. Shin, S. Lee, and Y. You, "A robust estimation of residual carrier frequency offset with I/Q imbalance in OFDM systems," *IEEE Trans. Veh. Technol.*, 2014, doi: 10.1109/TVT.2014.2311157.

[16] D. Mattera and M. Tanda, "Blind symbol timing and CFO estimation for OFDM/OQAM systems," *IEEE Trans. Wireless Commun.*, vol. 12, no. 1, pp. 268–277, Jan. 2013.

[17] M. Morelli and M. Moretti, "Joint maximum likelihood estimation of CFO, noise power, and SNR in OFDM systems," *IEEE Trans. Wireless Commun. Lett.*, vol. 2, no. 1, pp. 42–45, Feb. 2013.

[18] W. Zhang, Q. Yin, W. Wang, and F. Gao, "One-shot blind CFO and channel estimation for OFDM with multi-antenna receiver," *IEEE Trans. Signal Process.*, vol. 62, no. 15, pp. 3799–3808, Aug. 2014.

[19] H. Minn, V. Bhargava, and K. Letaief, "A robust timing and frequency synchronization for OFDM systems," *IEEE Trans. Wireless Commun.*, vol. 2, no. 4, pp. 822–839, July 2003.

[20] J. van de Beek, M. Sandell, and P. Borjesson, "ML estimation of time and frequency offset in OFDM systems," *IEEE Trans. Signal Process.*, vol. 45, no. 7, pp. 1800 –1805, Jul. 1997.

[21] T. Schmidl and D. Cox, "Blind synchronisation for OFDM," *Electronics Letters*, vol. 33, no. 2, pp. 113 –114, Jan. 1997.

[22] D. Toumpakaris, J. Lee, and H.-L. Lou, "Estimation of integer carrier frequency offset in OFDM systems based on the maximum likelihood principle," *IEEE Trans. Broadcast.*, vol. 55, no. 1, pp. 95 –108, Mar. 2009.

[23] *Digital Video Broadcasting (DVB); Framing structure, channel coding and modulation for digital terrestrial television*, ETSI EN 300 744, v1.6.1, Jan. 2009.

[24] IEEE, "802.11-2012 standard: Wireless LAN medium access control (MAC) and physical layer (PHY) specifications," Mar. 2012.

[25] S. Verdu, *Multiuser Detection*. Cambridge University, 1998.

[26] Y. Li, H. Minn, and J. Zeng, "An average Cramer-Rao bound for frequency offset estimation in frequency-selective fading channels," *IEEE Trans. Commun.*, vol. 9, no. 3, pp. 871–875, Mar. 2010.

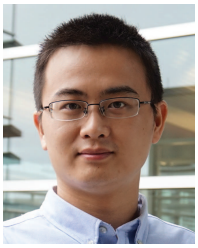

Qi Zhan received the B.E. and M.S. degree in Electrical Engineering from Huazhong University of Science and Technology in 2008 and 2011. He is currently working towards his Ph.D. degree in Electrical Engineering at the University of Texas at Dallas, TX, USA. His research interests are in the broad areas of wireless communications, signal processing, cognitive radio networks and advanced transmission schemes.

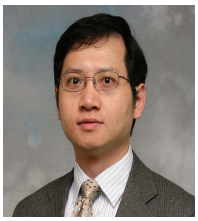

Hlaing Minn (S'99-M'01-SM'07) received the B.E. degree in electronics from the Yangon Institute of Technology, Yangon, Myanmar, in 1995; the M.Eng. degree in telecommunications from the Asian Institute of Technology, Pathumthani, Thailand, in 1997; and the Ph.D. degree in electrical engineering from the University of Victoria, Victoria, BC, Canada, in 2001. During JanuaryAugust 2002, he was a Postdoctoral Fellow with the University of Victoria. Since September 2002, he has been with the Erik Jonsson School of Engineering and Computer Science, University of Texas at Dallas, Richardson, TX, USA, where he is currently a Full Professor. His research interests include wireless communications, statistical signal processing, signal design, cross-layer design, cognitive radios, dynamic spectrum access and sharing, energy efficient wireless systems, next-generation wireless technologies and wireless healthcare applications.

Dr. Minn is an Editor of the IEEE TRANSACTIONS ON COMMUNICATIONS and the International Journal of Communications and Networks. He has served as a Technical Program Co-Chair for the Wireless Communications Symposium of the IEEE Global Communications Conference (GLOBECOM 2014) and the Wireless Access Track of the IEEE Vehicular Technology Conference (VTC2009Fall), as well as a Technical Program Committee Member for several IEEE conferences.